Strategies for optimisation of ^{177}Lu-octreotate therapy

Exploring local administration and combination therapy regimens

Viktor Sandblom

Department of Radiation Physics

Institute of Clinical Sciences

Sahlgrenska Cancer Center

Sahlgrenska Academy, University of Gothenburg

UNIVERSITY OF GOTHENBURG

Gothenburg 2019

Cover illustration by Johanna Allerth

Strategies for optimisation of ^{177}Lu-octreotate therapy – exploring local administration and combination therapy regimens

viktor.sandblom@gu.se

ISBN 978-91-7833-360-8 (PRINT)
ISBN 978-91-7833-361-5 (PDF)
http://hdl.handle.net/2077/58502

Printed in Gothenburg, Sweden 2019
Printed by BrandFactory

This is an insight into my life

This is a strange flight I'm taking

My true will carries me along

– *Martin Lee Gore (Depeche Mode)*

Abstract

Strategies for optimisation of ^{177}Lu-octreotate therapy – exploring local administration and combination therapy regimens

Viktor Sandblom

Department of Radiation Physics, Institute of Clinical Sciences, Sahlgrenska Cancer Center, Sahlgrenska Academy, University of Gothenburg, Sweden, 2019

Neuroendocrine tumours (NETs) are a group of heterogeneous tumour types that originate in hormone-producing organs. Patients with NETs are often diagnosed after the primary tumour has metastasised. One treatment option for these patients that has shown very promising results is systemic treatment using the radiolabelled somatostatin analogue ^{177}Lu-octreotate. However, the outcome of this treatment is currently restricted by healthy organs at risk.

The aim of this work was to optimise ^{177}Lu-octreotate therapy of NETs by investigating strategies based on local administration and on combination therapy regimens.

The feasibility of local treatment of liver metastases was evaluated by administering ^{177}Lu-octreotate via isolated hepatic perfusion (IHP) in a pig animal model. During IHP, the liver was completely isolated from the systemic circulation. An intraoperative gamma detector was evaluated for the purpose of determining ^{177}Lu activity concentration in vivo during treatment. This detector was also evaluated by assessment of its technical performance parameters using phantoms. In summary, the results showed that it could be feasible to treat patients with liver metastases from NETs with ^{177}Lu-octreotate via IHP. A relatively inhomogeneous uptake was obtained and to accurately quantify ^{177}Lu activity concentration using an intraoperative gamma detector, measurements may need to be performed at several positions over the liver.

In the combination therapy experiments, nude mice transplanted with NETs were treated with radiation therapy alone (as ^{177}Lu-octreotate or external beam radiotherapy) and in combination with one of the drugs gemcitabine, vandetanib, cabozantinib, or ganetespib. After treatment, tumour volume was followed and compared with that in control mice. Overall, combination treatment resulted in the largest decrease in tumour volume and the longest time to progression. The results indicated that additive, and sometimes synergistic, effects could be obtained when combining ^{177}Lu-octreotate with another drug for treatment of patients with NETs.

Keywords: Peptide receptor radionuclide therapy, PRRT, ^{177}Lu-octreotate, neuroendocrine tumours, optimisation, local administration, combination therapy

ISBN: 978-91-7833-360-8 (PRINT)
ISBN: 978-91-7833-361-5 (PDF)
E-publication: http://hdl.handle.net/2077/58502

Sammanfattning på svenska

Syftet med studierna i denna avhandling var att studera olika metoder för att förbättra målsökande strålbehandling med det radioaktiva läkemedlet ^{177}Lu-oktreotat (lutetium-177-oktreotat) för patienter med neuroendokrina tumörer.

Neuroendokrina tumörer är en cancertyp som kan uppkomma i kroppens hormonproducerande organ, t.ex. i tarmkanalen, lungorna eller levern. Vad som utmärker neuroendokrina tumörer från andra cancertyper är att de har en stor mängd av en viss sorts receptorer på sin cellyta. Detta möjliggör målsökande strålbehandling genom injektion av det radioaktiva läkemedlet ^{177}Lu-oktreotat. Läkemedlet består av två delar där radionukliden ^{177}Lu står för själva strålbehandlingen medan transportmolekylen oktreotat ser till att läkemedlet binder sig specifikt till neuroendokrina tumörceller. Ett problem vid behandlingen är att även friska organ i kroppen, främst njurar och benmärg, tar upp en viss mängd av läkemedlet, vilket kan leda till biverkningar om en för stor mängd ges. Denna begränsning gör det svårare att ge en tillräcklig mängd ^{177}Lu-oktreotat för att helt kunna bota patienter.

Studierna i denna avhandling har utförts som fem delarbeten. I arbete 1 och 2 studerades en ny metod för att ge ^{177}Lu-oktreotat-behandling lokalt till neuroendokrina tumörer i levern genom en s.k. isolerad leverperfusion där levern kirurgiskt kopplas bort från kroppens övriga blodcirkulation. Denna nya behandlingsmetod kan göra det möjligt att minimera upptag och biverkningar i friska organ. I arbete 1 utvärderades den tekniska prestandan för en strålningsdetektor avsedd för mätning av stråldosen till levern och dess tumörer under pågående behandling. Denna detektor, och behandlingsmetoden i stort, utvärderades vidare i arbete 2 där en tänkt patientsituation simulerades genom att behandla en gris.

I arbete 3, 4 och 5 studerades metoder där strålbehandling gavs tillsammans med ett av fyra icke-radioaktiva läkemedel i syfte att öka behandlingseffekten. Detta gjordes genom att behandla tumörbärande möss antingen med enbart strålning (som ^{177}Lu-oktreotat eller extern strålbehandling) eller strålning i kombination med ett annat läkemedel för att sedan jämföra effekten av dessa behandlingar.

Sammanfattningsvis visade resultaten att 1) isolerad leverperfusion med ^{177}Lu-oktreotat är en ny och lovande metod för att förbättra målsökande strålbehandling av neuroendokrina tumörer i levern, och 2) effekten av strålbehandling på neuroendokrin tumörvävnad kan ökas genom att kombinera behandlingen med ett annat läkemedel, både med avseende på tumörvolym och effektens varaktighet.

List of papers

This thesis is based on the following studies, referred to in the text by their Roman numerals.

I. Sandblom V, Ståhl I, Olofsson Bagge R, Forssell-Aronsson E. **Evaluation of two intraoperative gamma detectors for assessment of ^{177}Lu activity concentration in vivo**. EJNMMI Physics 2017; 4(3): 1-15.

II. Sandblom V, Ståhl I, Hansson C, Olofsson Bagge R, Forssell-Aronsson E. **Local treatment of liver metastases by administration of ^{177}Lu-octreotate via isolated hepatic perfusion – a preclinical simulation of a novel treatment strategy**. Submitted.

III. Sandblom V, Spetz J, Shubbar E, Montelius M, Ståhl I, Swanpalmer J, Nilsson O, Forssell-Aronsson E. **Gemcitabine potentiates the anti-tumour effect of radiation on medullary thyroid cancer**. Submitted.

IV. Sandblom V, Spetz J, Shubbar E, Montelius M, Ståhl I, Swanpalmer J, Nilsson O, Forssell-Aronsson E. **Increased therapeutic effect on medullary thyroid cancer using a combination of radiation and tyrosine kinase inhibitors**. Manuscript.

V. Hofving T, Sandblom V, Arvidsson Y, Shubbar E, Altiparmak G, Swanpalmer J, Almobarak B, Elf AK, Johanson V, Elias E, Kristiansson E, Forssell-Aronsson E, Nilsson O. **^{177}Lu-octreotate therapy for neuroendocrine tumours is enhanced by Hsp90 inhibition**. Endocrine-Related Cancer 2019; 26(4): 437-449.

Selection of related presentations

I. Sandblom V, Ståhl I, Olofsson Bagge R, Forssell-Aronsson E. **Evaluation of the possibility of using intraoperative gamma probe measurements for determining ^{177}Lu-octreotate activity concentration in vivo**. 27th Annual Congress of the European Association of Nuclear Medicine, Gothenburg, Sweden, October 18-22, 2014.

II. Sandblom V, Ståhl I, Olofsson Bagge R, Forssell-Aronsson E. **Determination of ^{177}Lu-octreotate activity concentration in vivo using intraoperative gamma probes – a comparative study**. Swedish Cancer Society Winter Meeting, Umeå, Sweden, January 22-23, 2015.

III. Sandblom V, Spetz J, Swanpalmer J, Forssell-Aronsson E. **Treatment of medullary thyroid cancer using a combination of radiation and gemcitabine**. 62nd Annual International Meeting of the Radiation Research Society, Waikoloa Village, Hawaii, USA, October 15-19, 2016.

IV. Sandblom V, Spetz J, Shubbar E, Swanpalmer J, Forssell-Aronsson E. **Combination therapy of medullary thyroid cancer using radiation and vandetanib**. 30th Annual Congress of the European Association of Nuclear Medicine, Vienna, Austria, October 21-25, 2017.

V. Sandblom V, Ståhl I, Hansson C, Olofsson Bagge R, Forssell-Aronsson E. **Administration of ^{177}Lu-octreotate via isolated hepatic perfusion – an experimental pilot study of activity concentration measurements in liver of pig**. National Meeting of Medical Physics, Västerås, Sweden, November 15-17, 2017.

VI. Sandblom V, Spetz J, Shubbar E, Ståhl I, Swanpalmer J, Forssell-Aronsson E. **Vandetanib may act as a radiosensitiser for ^{177}Lu-octreotate treatment of medullary thyroid cancer**. 2nd European Congress of Medical Physics, Copenhagen, Denmark, August 22-25, 2018.

Table of contents

Abbreviations

ANOVA	Analysis of variance
ATA	American Thyroid Association
Bq	Becquerel
Cd	Cadmium
cps	Counts per second
Cs	Caesium
CT	Computed tomography
CV	Coefficient of variation
DNA	Deoxyribonucleic acid
EBRT	External beam radiotherapy
FDA	Food and Drug Administration
FOV	Field-of-view
FWHM	Full-width-at-half-maximum
Ga	Gallium
Gy	Gray
H&E	Haematoxylin and eosin
HAE	Hepatic artery embolisation
HSP	Heat shock protein
I	Iodine
i.p.	Intraperitoneal
i.v.	Intravenous
IGD	Intraoperative gamma detector
IHC	Immunohistochemical
IHP	Isolated hepatic perfusion
In	Indium
ITLC	Instant thin layer chromatography
LAR	Long-acting repeatable
Lu	Lutetium
MEN2	Multiple endocrine neoplasia type 2
MIBG	Metaiodobenzylguanidine
MIRD	Medical Internal Radiation Dose
MT	Masson's trichrome
MTC	Medullary thyroid cancer
mTOR	Mammalian target of rapamycin
Na	Sodium
NAMPT	Nicotinamide phosphoribosyltransferase
NET	Neuroendocrine tumour
OS	Overall survival
P	Phosphorus

PARP-1	Poly [ADP-ribose] polymerase 1
PET	Positron emission tomography
PFS	Progression-free survival
PRRT	Peptide receptor radionuclide therapy
RE	Radioembolisation
RET	Rearranged during transfection
RFA	Radiofrequency ablation
RTV	Relative tumour volume
SD	Standard deviation
SEM	Standard error of the mean
SI-NET	Small-intestine neuroendocrine tumour
SIRT	Selective internal radiation therapy
SPECT	Single-photon emission computed tomography
SST	Somatostatin
SSTR	Somatostatin receptor
TACE	Trans-arterial chemoembolisation
TAE	Trans-arterial embolisation
TARE	Trans-arterial radioembolisation
Tc	Technetium
Te	Tellurium
TKI	Tyrosine kinase inhibitor
Tl	Thallium
VEGF	Vascular endothelial growth factor
Y	Yttrium

1 Introduction

This thesis focuses on two strategies for optimisation of ^{177}Lu-octreotate therapy: 1) local drug administration in order to spare healthy organs at risk, and 2) combination therapy regimens.

1.1 Neuroendocrine tumours

Neuroendocrine tumours (NETs) are a heterogeneous group of slow-growing tumour types that originate in the endocrine or nervous system [1, 2]. The most common site of origin is the gastrointestinal tract, followed by the lungs, pancreas, liver, thymus and thyroid. NETs often secrete a large amount of hormones resulting in the so-called carcinoid syndrome with diarrhea and flushing as common symptoms. Patients with NET experience a lower quality of life compared with the general population [3]. Because of the endocrine origin, NETs frequently overexpress somatostatin (SST) receptors (SSTRs) which can serve as molecular targets for systemic therapy [4, 5]. SSTRs occur in five different subtypes (SSTR1-5) and the relative expression of these subtypes can affect the choice of drug.

The incidence of NETs has increased over the last few decades from about 1 to 5 cases per 100,000 people, and is believed to be around 8 per 100,000 today [6]. Generally, the primary tumour is small and give relatively vague symptoms initially. Therefore, many patients have metastatic spread at the time of diagnosis and consequently a worse prognosis. The survival is strongly dependent on tumour stage and grade but also site of origin. It is difficult to give an exact number but reports on 5-year survival vary between about 50-80% and 20-60% for localised and metastatic disease, respectively [1, 6-8].

Small-intestine NETs (SI-NETs) constitute a type of NETs that often originate in the ileum of the small intestine [8, 9]. The characteristics of SI-NETs are similar to those associated with NETs in general, *e.g.*, SSTR overexpression, slow growth rate, and vague initial symptoms. In addition to SSTRs, SI-NETs also express chromogranin A, synaptophysin, and serotonin, which can be used as indicators for the disease.

Medullary thyroid cancer (MTC) is another example of a cancer that belongs to the family of NETs. There are several types of thyroid cancers, but only a small fraction (1-2%) of all thyroid cancers are diagnosed as medullary thyroid cancer [10]. In contrast to other types of thyroid cancer, MTC originates from the parafollicular C-cells of thyroid, resulting in a hormone-producing feature

characteristic for NETs. MTC can occur either sporadically or as a hereditary form often part of the so-called multiple endocrine neoplasia type 2 (MEN2) syndrome. In addition to overexpression of SSTRs, mutations in the proto-oncogene rearranged during transfection (RET) is common in MTC, further enabling the use of targeted therapies [11].

1.1.1 Treatment of neuroendocrine tumours

The primary treatment for patients with NETs is surgery and many patients are operated with curative intent [12]. However, due to the high prevalence of metastatic spread, additional treatment is needed for many patients. There are several treatment options for patients with metastatic disease. Most of these patients receive one or several types of systemic therapy following surgery. If the metastases are confined to the liver, some kind of liver-specific treatment can be an option.

1.1.1.1 Liver-specific treatments

The gastrointestinal tract is the most common site of origin for NETs. Consequently, metastatic spread to the liver is common because of the anatomical structure of the circulation system. For patients with liver-dominant disease, several liver-specific treatments are available, including trans-arterial embolisation (TAE) [13], trans-arterial chemoembolisation (TACE) [14], radioembolisation (RE) [15, 16], radiofrequency ablation (RFA) [17], and liver or multivisceral transplantation [18]. Most of these treatments utilise the fact that the liver has two main blood supplies – the hepatic artery and the portal vein – and that healthy liver tissue receives most of its blood and nutrients from the portal vein, while many malignancies, *e.g.* liver metastases from NETs, are instead mainly supplied by the hepatic artery.

In TAE, also known as hepatic artery embolisation (HAE), the hepatic artery is occluded by injection of a blocking agent (*e.g.* plastic particles, glue, or metal coils) resulting in ischemia and necrosis in the tumours. TACE is similar to TAE, but instead of simply shutting of the blood supply, the blocking agent particles are also coated with a chemotherapeutic drug. Hence, when these particles are injected into the liver via the hepatic artery, the tumours will be attacked in several ways. Since the hepatic artery is used for the injection, the tumours will be more affected than the healthy normal tissue. The radiotherapeutic equivalent of TACE is RE, in which small radioactive glass or resin spheres (most commonly containing ^{90}Y) are used instead of particles coated with chemotherapeutic drugs. These radioactive spheres lodge in the small vessels of the tumour resulting in local irradiation of the tumour cells. This treatment is also known as selective internal radiation therapy (SIRT) or trans-arterial radioembolisation (TARE).

Another option for treatment of liver metastases from NETs is RFA. Unlike the embolisation procedures described above, RFA is not based on the difference in blood supply for tumours and healthy liver tissue. Instead, a needle-like probe is placed inside each tumour to be treated and a radiofrequency alternating current is used to increase the temperature inside the tumour leading cell death.

1.1.1.2 Systemic therapy

When NETs have spread beyond the liver, which is not uncommon, some kind of systemic therapy is needed. Several systemic drugs are available for NETs but most of these are associated with side effects and sometimes the toxicity can overweigh the benefits of treatment.

SST analogues have shown positive effects on symptom control for many NETs. Natural SST has a very short biological half-life in patients. Therefore, two long-acting formulations of SST analogues have been developed and evaluated in clinical phase III studies, namely octreotide long-acting repeatable (LAR) and lanreotide autogel [19, 20]. These drugs show similar efficiency and are routinely used as first-line systemic treatment for many NETs today, especially for those that are functionally active [12].

Many other systemic drugs have also been evaluated for treatment of NETs. Interferon alpha can be used as second-line therapy after SST analogues, mainly for symptomatic control but it has also shown inhibition of tumour growth in some patients [21]. Telotristat ethyl is a more recent drug that can be used to reduce hormonal symptoms from NETs [22]. Everolimus is another option for treatment of NETs, especially for pancreatic NETs for which everolimus is recommended for first- or second-line treatment following the results of a large phase III study [23]. Furthermore, several tyrosine kinase inhibitors (TKIs) have shown very promising results in NETs, including sunitinib for pancreatic NETs as well as vandetanib and cabozantinib for MTC [24-26]. Vandetanib and cabozantinib are both approved by the Food and Drug Administration (FDA) for treatment of patients with metastatic MTC and also recommended by the American Thyroid Association (ATA) as single-agent first-line therapy in these patients [10].

Chemotherapy can also be a treatment option for patients with NETs even though one or several of the above mentioned targeted therapies are preferred. Chemotherapy are mainly used for more aggressive high-grade NETs or those that are SSTR negative. A combination of streptozotocin, doxorubicin and 5-fluorouracil has been an established therapy but temozolomide with capecitabine

is now gaining popularity [27, 28]. Gemcitabine is another chemotherapeutic drug that has been evaluated both for MTC and other NETs [29-31].

Lastly, one of the most successful and promising systemic treatment options for patients with NETs is peptide receptor radionuclide therapy (PRRT) using ^{177}Lu-octreotate. In 2010, a large multicenter phase III trial was initiated. Preliminary results are now available which have led to the approval of ^{177}Lu-octreotate for certain NETs. PRRT is described more in detail in chapter 1.2.1.

1.2 Radionuclide therapy

In radionuclide therapy, the ionising radiation emitted through the decay of radioactive atoms (also called radionuclides) is used to treat different medical conditions, *e.g.* cancer. The first systemic radionuclide therapy experiments were performed in 1913 by Frederick Proescher who injected patients with soluble radium salts [32]. A few decades later, new radionuclides were introduced. In 1936, ^{32}P and ^{24}Na were first used to treat leukaemia and polycythaemia vera [33]. During the 1940s, ^{131}I was first used for several thyroid-related conditions, *e.g.* hyperthyroidism and thyroid cancer. Some of these early examples of radionuclide therapy are still in clinical use today.

The development of carrier molecules has been a landmark for radionuclide therapy. Early uses included monoclonal antibodies, which had a substantially lower specific uptake in tumours than many of the much smaller carrier molecules commonly used today. In the 1980s, after ^{131}I had been chemically bound to metaiodobenzylguanidine (MIBG), the first clinical experiments of using ^{131}I for treatment patients with NETs were performed [34, 35]. After ^{111}In had been bound to the peptide octreotide in the early 1990s, and a high specific uptake of this compound in NETs had been demonstrated, the field of PRRT began to emerge [36, 37].

1.2.1 Peptide receptor radionuclide therapy

PRRT is a term used to describe treatments in which radionuclides are bound to small peptides that bind with high affinity to SSTRs and used to treat NETs. Two commonly used peptides are the SST analogues octreotide and octreotate. These peptides are very similar but have minor differences in amino acid composition and octreotate has a higher affinity for SSTR2 [38]. The first clinical PRRT experiments were performed in the early 1990s using ^{111}In-octreotide [39-41]. These early studies showed a favourable effect on hormone-related symptoms but tumour regression was rarely seen. A few years later, ^{111}In was substituted by beta-emitting radionuclides ^{90}Y and ^{177}Lu [42-44]. Initial therapeutic results of ^{90}Y-

octreotide and ^{177}Lu-octreotate were very encouraging and demonstrated improved rates of tumour regression compared with ^{111}In-octreotide, as well as a reduction of the side effects previously associated with ^{111}In-octreotide such as myelodysplastic syndrome and leukaemia. However, severe kidney toxicity was noted in some patients after ^{90}Y-octreotide therapy which lead to the introduction of kidney-protecting agents for PRRT [45]. Following these developments, many patients have been successfully treated with ^{90}Y-octreotide and ^{177}Lu-octreotate over the past two decades. In recent years, ^{177}Lu-octreotate have gained increasing popularity over ^{90}Y-octreotide, partly because of the lower kidney toxicity associated with ^{177}Lu-octreotate [46].

Today, ^{177}Lu-octreotate (full name Lutetium-177-[DOTA^0, Tyr^3]-octreotate) therapy is a well-established treatment for patients with NETs in many centres worldwide [47-57]. Treatment is given according to a standardised protocol originally developed at the Erasmus Medical Center in Rotterdam [58]. First, to avoid saturation of SSTRs, systemic treatment with SST analogues is usually interrupted about 4-6 weeks before start of ^{177}Lu-octreotate treatment. Then, ^{177}Lu-octreotate is given in cycles, with an interval of about 6-10 weeks between cycles, to allow bone marrow and other healthy organs at risk time to recover. During each cycle, 3.7 or 7.4 GBq ^{177}Lu-octreotate is administered as an intravenous (i.v.) infusion over 30 minutes. To reduce the uptake in and exposure of the kidneys, positively charged amino acids, usually lysine and arginine, are administered together with the ^{177}Lu-octreotate infusion. The number of cycles, and thus the total amount of ^{177}Lu-octreotate, given to each patient is restricted by healthy organs at risk. Treatment is discontinued when the absorbed dose has reached 23-28 Gy to the kidneys or 2 Gy to the bone marrow, whichever comes first. This restriction usually results in 4-6 treatment cycles.

^{177}Lu-octreotate was recently approved, under the marketing name Lutathera®, for the treatment of patients with advanced metastatic midgut NETs both in the USA and in Europe. This approval followed the results of the first randomised controlled trial (NETTER-1). In that study, ^{177}Lu-octreotate was compared to octreotide LAR (current first-line therapy for metastatic NETs) and demonstrated significantly prolonged progression-free survival (PFS) and improved quality of life [59, 60]. Final results on overall survival (OS) are not yet published. In the prescribing information for Lutathera®, a fixed treatment protocol including 4 cycles of 7.4 GBq is specified.

1.3 NET-related radionuclides

When radionuclides are used for therapy, a high emission yield of particles with short range, *e.g.* electrons, and a low photon contribution is required to achieve a

high absorbed dose locally [61]. For example, the two most commonly used radionuclides for PRRT, ^{90}Y and ^{177}Lu, emit primarily electrons. Favourable properties for localisation and diagnosis can instead be achieved by using a radionuclide with a high emission yield of photons, or positrons resulting in annihilation photons. Until recently, a SPECT scan with ^{111}In-octreotide has been the gold standard for image-based diagnosis of NETs [62]. This imaging technique is now being replaced by PET scans with ^{68}Ga-labeled SST analogues due to their superior ability to detect NET lesions [63, 64]. Table 1 lists physical properties of the radionuclides most commonly used for diagnosis and/or treatment of NETs.

Table 1. Physical properties of radionuclides most commonly used for diagnosis and/or treatment of NETs [65]

			Average energy per decay (keV)		
Radionuclide	Main purpose	Half-life	Electrons	Positrons	Photons
^{68}Ga	Diagnosis	67.7 min	0.560	737	949
^{90}Y	Therapy	2.67 d	933		<0.01
^{111}In	Diagnosis	2.80 d	34.8		406
^{177}Lu	Therapy	6.65 d	148		35.1

1.4 Optimisation of ^{177}Lu-octreotate therapy

Even though ^{177}Lu-octreotate therapy has shown a profound benefit for patients with NETs since its introduction, few patients achieve complete remission and optimisation of ^{177}Lu-octreotate therapy is warranted. Several potential strategies for optimisation of PRRT have been suggested, *e.g.*, methods to increase SSTR expression, choice of radionuclide and carrier molecule, the use of kidney-blocking or radio-protecting agents, fractionation schedule, local administration, or combination therapy [66]. These strategies can be categorised into one of two main approaches, to 1) reduce side effects on healthy organs at risk, or 2) increase the therapeutic effect on tumour tissue. This thesis focuses on optimisation of ^{177}Lu-octreotate therapy by exploring two of the suggested strategies; namely local administration and combination therapy regimens.

1.4.1 Local administration

The main purpose of local administration is to reduce the exposure of healthy organs at risk. This can be especially useful for liver metastases from NETs. The

previously discussed liver-specific treatments are a few examples of local administration techniques. However, these methods are not based on PRRT. Intra-arterial injection directly into the liver is one technique that has been tested for PRRT [67, 68]. The goal of an intra-arterial injection is that a large part of the administered amount will bind to SSTRs in liver metastases during the first passage through the liver, leading to a reduced uptake in healthy organs at risk. To further reduce the systemic exposure, the technique of isolated hepatic perfusion (IHP) could be utilised.

1.4.1.1 Isolated hepatic perfusion (IHP)

During IHP, the liver is completely isolated from the systemic circulation, allowing high doses of drugs to be administered to the liver with minimal systemic exposure [69]. Before the isolated perfusion circuit is established, the femoral and external jugular veins are connected to an external pump creating a percutaneous bypass from the lower extremity around the liver. Then, the portal vein is clamped and the hepatic artery and the inferior caval vein are cannulated and connected to a heart-lung machine, isolating the liver from the systemic circulation (Figure 1). The liver can then be perfused by blood containing high concentrations of drugs. After 60 minutes, the liver is thoroughly rinsed and the procedure ends by restoration of the systemic circulation. Today, IHP with the chemotherapeutic drug melphalan is clinically used to treat liver metastases from malignant melanoma and colorectal cancer, but has also been evaluated for NETs [70-72].

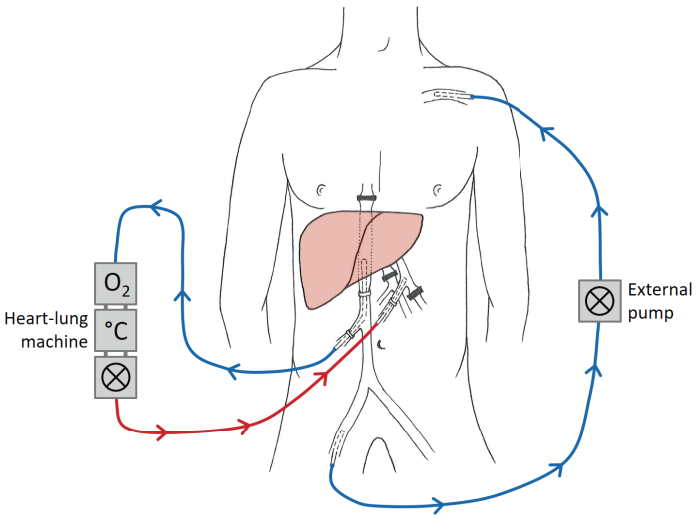

Figure 1. Schematic overview of the setup for the IHP procedure. Illustration by Johanna Allerth

IHP has not yet been used together with radionuclide therapy. This could now be possible due to the development of disposable components that prevent

radioactive contamination of the heart-lung machine. By administering ^{177}Lu-octreotate using the IHP technique in order to treat liver metastases from NETs, the exposure of kidneys and bone marrow (which are the main organs at risk for systemic ^{177}Lu-octreotate therapy) might be strongly reduced. This administration technique would also lead to an increased concentration of ^{177}Lu-octreotate in the blood circulating through the IHP circuit. For this proposed procedure, the healthy liver tissue would instead be the main organ at risk, because of the isolation from the systemic circulation and the high concentration of ^{177}Lu-octreotate present in the liver. Therefore, the absorbed dose to the liver has to be closely monitored so that the perfusion can be ended if needed to avoid negative side effects. It would also be important to determine the absorbed dose to liver metastases, as well as the exposure of organs and other tissues outside the isolated perfusion circuit, since a certain degree of leakage of ^{177}Lu-octreotate could occur either during the IHP or after the liver has been reconnected to the systemic circulation. All this requires accurate quantification of ^{177}Lu activity concentration in vivo. One option for this quantification could be to use an intraoperative gamma detector (IGD).

IGDs are small hand-held instruments for detection of gamma radiation [73]. They are designed to be used for radioguided surgery, where the purpose is to find and surgically remove lesions during surgery after an injection of a diagnostic radiotracer based on *e.g.* ^{99m}Tc or ^{111}In. One example of radioguided surgery is the location of NETs after an injection of ^{111}In-octreotide [74, 75]. Since ^{177}Lu emits both electrons and photons (Table 1), it is possible that ^{177}Lu activity concentration could be quantified in vivo using an IGD. Over the last few decades, the technical performance of IGDs have been evaluated, such as sensitivity, response linearity, and spatial resolution [76-83]. However, most of these evaluations were made for diagnostic situations involving low amounts of activity of radionuclides other than ^{177}Lu. For the proposed treatment technique of administering ^{177}Lu using IHP, a much higher amount of activity would be used compared with the diagnostic situation.

Before the proposed treatment technique can be used clinically for patients, it is important to evaluate the possibility of using IGD measurements to quantify ^{177}Lu activity concentration in vivo in this therapeutic situation. As a first step, a technical performance evaluation by phantom measurements of ^{177}Lu is needed. It will also be necessary to simulate the clinical situation in order to study uptake and distribution of ^{177}Lu in healthy liver tissue, to estimate the radiation exposure of the staff involved, and to further evaluate the quantification ability of the IGD.

1.4.2 Combination therapy

Combination therapy is a promising and growing area of PRRT optimisation [66]. When radiation interacts with a cell, it can deliver all or part of its energy to the deoxyribonucleic acid (DNA) in the cell nucleus, leading to radiation-induced DNA damage. These damages also occur indirectly when free radicals, created by the radiation, interacts with the DNA. Radiation-induced DNA damage is followed by cellular responses such as cell cycle arrest, DNA repair, senescence, apoptosis, and mitotic catastrophe [84]. If ^{177}Lu-octreotate is combined with a substance that affect such responses, leading to an interaction between the effects of the two substances, it is possible that the anti-tumour effect from the ionising radiation can be increased in a synergistic manner. This interaction is usually referred to as radiosensitisation [85].

Apart from potentially resulting in a synergistic anti-tumour effect, combination therapy can offer several important benefits for cancer patients (Figure 2) [86]. Firstly, if two drugs with different toxicity profiles are used, then the total amount of treatment can be increased compared with either monotherapy. Secondly, many cancer patients develop drug resistance with time, and for these patients, the switch to a new treatment can be an important next step in their treatment. Also, if two drugs are administered at the same time, it is possible that one of the drugs can inhibit development of resistance to the other. Thirdly, the use of multiple drugs could be crucial to be able to effectively treat heterogeneous tumours in which only part of the cells respond to a certain drug. The same argument can be made for multiple tumours within a patient, for example if liver metastases respond differently than bone metastases. Lastly, given that there is a large individual variation between patients, the use of combination therapy gives each patient a better chance that at least one drug will be effective [87].

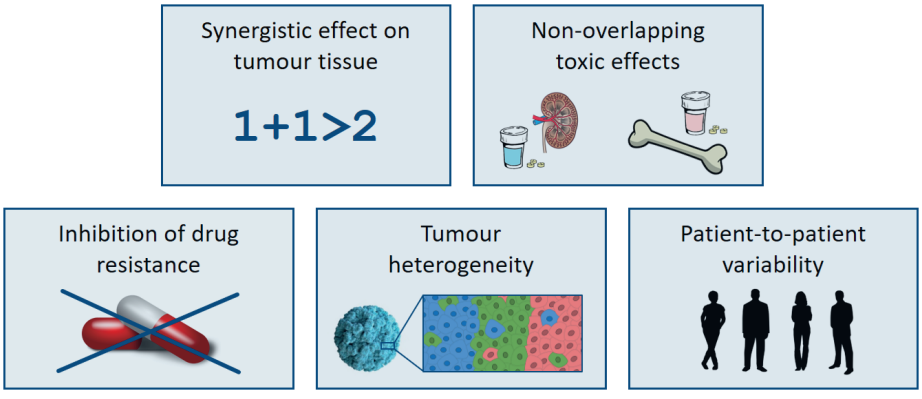

Figure 2. Overview of some potential benefits of combination therapy [86, 87]

There are several clinical examples of combination therapy involving PRRT for the treatment of NETs. One of the first combinations evaluated was ^{177}Lu-octreotate plus capecitabine [88-90]. The addition of temozolomide to this combination has also been evaluated [91, 92]. In some cases, the infusion of 5-fluorouracil has been used instead of its oral prodrug capecitabine [50, 93]. Results indicate that combination therapy can increase PFS and OS compared with only PRRT. More recently, the combination of ^{177}Lu-octreotate plus everolimus has also been evaluated but many patients required dose reduction or treatment discontinuation due to treatment-related side effects [94]. The development of new and efficient treatment combinations for NETs is important to further optimise the outcome of PRRT. In preclinical studies, many drugs are being evaluated in combination with radiation therapy for NETs and other cancer types. A few candidates are presented below.

1.4.2.1 Gemcitabine

Gemcitabine is a chemotherapeutical nucleoside analogue that has shown anti-tumour effect in many cancer types including MTC [30, 95]. The mechanism of action for gemcitabine starts with activation by phosphorylation resulting in the active metabolites gemcitabine diphosphate and triphosphate [96, 97]. These metabolites are responsible for the cytotoxic effect by incorporation in the DNA during DNA synthesis leading to cell cycle arrest or apoptosis, and by interfering with the enzyme ribonucleotide reductase involved in DNA synthesis and repair.

In preclinical studies, gemcitabine has a well-documented radiosensitising effect on many cancer types [98-102]. The combination of external beam radiotherapy (EBRT) and gemcitabine has also been evaluated in many clinical studies, most commonly for pancreatic cancer [103-107]. Therefore, gemcitabine is an interesting candidate for combination therapy with PRRT for NETs.

1.4.2.2 Vandetanib and cabozantinib

Vandetanib and cabozantinib are targeted drugs belonging to the family of TKIs. One target for these drugs is the RET proto-oncogene, frequently mutated in MTC [11]. In addition, vandetanib and cabozantinib also target receptors for the signal protein vascular endothelial growth factor (VEGF) which are commonly overexpressed in MTC [108]. Inhibition of tyrosine kinases related to these targets leads to the main anti-tumour effect.

As previously mentioned, vandetanib and cabozantinib are both approved for systemic treatment of metastatic MTC following the results of two large phase III trials [24, 25]. Given the promising clinical results and the recommendation by the ATA of using vandetanib and/or cabozantinib as first-line systemic therapy

for metastatic MTC [10], it would be very interesting to evaluate the possibility of achieving an increased effect on MTC by combination therapy with PRRT.

1.4.2.3 Ganetespib

Ganetespib is a novel targeted drug acting as an inhibitor of heat shock protein (HSP) 90 [109]. HSP90 is a molecular chaperone that regulates normal folding, stability, and function of proteins [110]. Some of these proteins are required for tumour cell survival and growth, and consequently, HSP90 is upregulated in several types of cancer [111, 112]. Therefore, inhibition of HSP90 offers a new and promising therapeutic approach for cancer therapy.

Ganetespib is currently being evaluated in clinical trials. Results from several recent phase I-II trials including various cancer types show that ganetespib is associated with manageable toxicity and preliminary disease control rates (stable disease or better response) of about 25-30% [113-116]. In many preclinical studies, ganetespib has been shown to have a radiosensitising effect in various cancer cell lines [117-120]. Further investigations of this radiosensitising effect in NETs would be interesting in order to evaluate ganetespib for combination therapy with PRRT.

2 Aims

The overall aim of this work was to investigate strategies to optimise ^{177}Lu-octreotate therapy of neuroendocrine tumours based on local administration (Papers I-II) and on combination therapy regimens (Papers III-V).

The specific aims were:

- to evaluate the ability of two intraoperative gamma detectors to quantify ^{177}Lu activity concentration in vivo by measuring performance parameters, such as sensitivity, response linearity, and spatial resolution, using phantoms (Paper I)

- to evaluate the feasibility of using ^{177}Lu-octreotate therapy administered via isolated hepatic perfusion by simulating the clinical situation in a pig model (Paper II)

- to investigate the effect of combining radiation treatment with gemcitabine for medullary thyroid cancer in a mouse model (Paper III)

- to investigate the effect of combining radiation treatment with tyrosine kinase inhibitors vandetanib or cabozantinib for medullary thyroid cancer in a mouse model (Paper IV)

- to investigate the effect of combining ^{177}Lu-octreotate treatment with ganetespib for small-intestine neuroendocrine tumours in a mouse model (Paper V)

3 Materials and Methods

3.1 Radiopharmaceutical (Papers I-III and V)

^{177}Lu-octreotate was prepared according to the manufacturer's instructions (IDB Holland BV, the Netherlands). The fraction of peptide-bound ^{177}Lu was determined by instant thin layer chromatography (ITLC SG, PALL Corporation, USA). This fraction was over 99% in all experiments. The stock solution of ^{177}Lu-octreotate was diluted using saline solution to the desired concentration for each experiment. ^{177}Lu activity was determined using a well-type ionisation chamber (CRC-15R, Capintec, USA).

3.2 Local administration of ^{177}Lu-octreotate (Papers I-II)

By administering ^{177}Lu-octreotate via IHP, the uptake in and exposure of healthy organs at risk could be strongly reduced. To evaluate whether an IGD could be used to estimate ^{177}Lu activity concentration in tissues during this proposed procedure, performance parameters of two commercially available IGDs were assessed using phantoms containing ^{177}Lu. To further evaluate the feasibility of the proposed procedure, a clinical situation was simulated using a pig model.

3.2.1 Phantom measurements (Paper I)

Measurements were performed using sources and phantoms containing ^{177}Lu. The performance parameters examined were response linearity, sensitivity, spatial resolution and its depth dependence, organ thickness dependence, and tumour detectability.

The two IGDs evaluated were the Gamma Finder II (World of Medicine GmbH, Germany) and the Navigator GPS (Dilon Diagnostics, USA), hereafter called detector A and B, respectively. Detector A is a scintillation detector containing a CsI(Tl) crystal and detector B is a semiconductor detector containing a CdTe crystal. Both detectors are equipped with tungsten collimators. Detailed dimensions of the detectors can be seen in Figure 3. Detector A has a non-adjustable low-energy threshold of 110 keV. Detector B has a set of pre-defined energy windows suited for measurements of different diagnostic radionuclides (^{99m}Tc, ^{111}In, ^{125}I, and ^{131}I). A 20% energy window centered over the ^{99m}Tc peak at 141 keV (range 112-169 keV) was used for all detector B measurements.

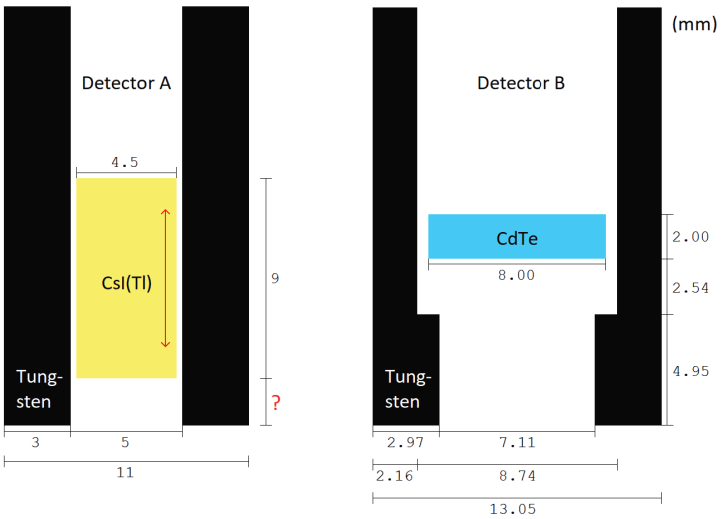

Figure 3. Schematic view of the geometrical design of the two IGDs evaluated. Information about the distance from the crystal to the end of the collimator was not available for detector A, indicated by the question mark and the arrow inside the crystal. Distances in mm. Figure adapted with modification from Paper I

Response linearity and sensitivity was assessed using point sources of increasing activity. For each activity, the count rate as counts per second (cps) was determined. The sensitivity was calculated as the slope of the trend line fitted to the data obtained.

Spatial resolution and its depth dependence was assessed using a line source placed at different depths (0-80 mm) in a block phantom of tissue-equivalent plastic. The detector was placed at the surface of the phantom and moved perpendicularly across the line source. The spatial resolution was determined as full-width-at-half-maximum (FWHM) of the line profiles obtained.

Organ thickness dependence was assessed using a gel phantom consisting of a stack of 2% agarose gel blocks containing a homogeneous activity distribution. The detector was placed at the surface of the gel phantom and the count rate for different thicknesses (10-150 mm) was determined.

Tumour detectability was assessed using a tumour phantom created by placing a gel sphere (simulating a tumour) at the surface of the gel phantom described above (simulating the background). The tumour spheres (5-20 mm diameter) contained 2-30 times higher activity concentration than the background blocks, and values were assumed to be relevant for clinical situations [121, 122]. The number of counts over the tumour sphere (C_T) and over the background (C_{Bgr}) was measured (Figure 4).

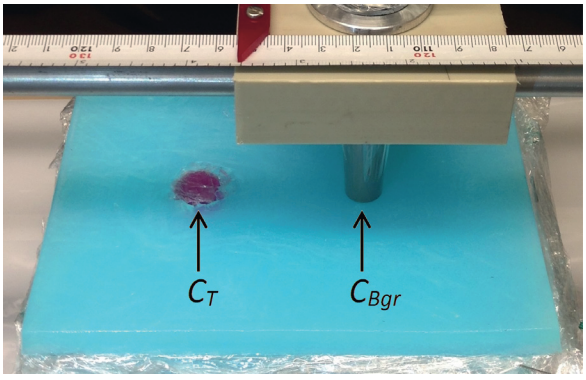

Figure 4. Measurement setup for the assessment of tumour detectability. Figure adapted with modification from Paper I

For the assessments of organ thickness dependence and tumour detectability, statistical analyses were performed to find statistically significant differences between two given signal intensities, C_1 and C_2. The standard deviation (SD) of the difference between the signals, $\sigma(C_1\text{-}C_2)$, was calculated:

$$\sigma(C_1 - C_2) = \sqrt{C_1 + C_2} \quad (1)$$

Then, differences between C_1 and C_2 were considered statistically significant ($p<0.05$) if they exceeded two SDs of the difference, *i.e.* if $C_1\text{-}C_2 > 2\times\sigma(C_1\text{-}C_2)$. For the assessment of organ thickness, the signal intensity at each thickness was compared with the signal intensity at the largest thickness (150 mm). For the assessment of tumour detectability, C_T was compared with C_{Bgr} for each tumour-to-background ratio and tumour size.

3.2.2 Simulation of the clinical situation (Paper II)

To simulate the clinical situation, a healthy pig was prepared for surgery. The IHP procedure was performed ex vivo to avoid any potential risk of contaminating the entire pig. After the liver had been connected to a heart-lung machine, it was removed and placed in a bowl and the pig was euthanised. The perfusion circuit was established according to a standard IHP procedure with one exception – the portal vein was used for the perfusion instead of the hepatic artery [69]. The perfusion was started and once a steady blood flow had been established, 490 MBq ^{177}Lu-octreotate was added to the system. After 60 minutes, the perfusion was stopped and the liver was rinsed with Ringer's solution (Ringer Acetat, Baxter Medical AB, Sweden). This study was approved by the Ethical Committee on Animal Experiments in Gothenburg, Sweden.

During the perfusion and rinsing, two detectors were used to monitor ^{177}Lu activity concentration. Detector B was positioned over the liver and a collimated NaI(Tl) scintillation detector (Scintibloc type 51 SL 12 no. 7775, Saint-Gobain S.A., France) connected to a locally developed software (MedicView, Systemdata, Sweden) was positioned over the circuit tube (Figure 5). In addition, all staff members present in the operating room wore personal dosimeters (Harshaw TLD, Thermo Scientific, USA) registering both whole body and extremity exposure. A hand-held intensimeter (RNI 10/SR Intensimeter, Nuklidtech Sweden AB, Sweden) was used to measure the exposure environment at locations where a high radiation dose rate was expected.

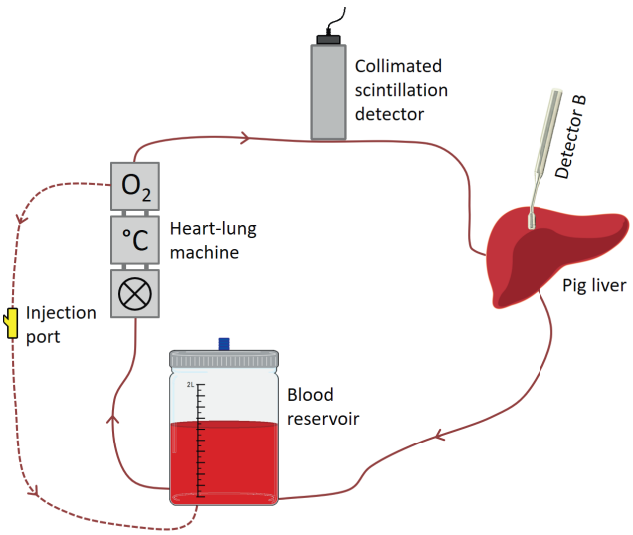

Figure 5. Experimental setup for the IHP simulation. The blood reservoir was sealed inside a 10 mm thick lead cylinder (not shown). The circuit included an injection port for safe administration of substances into the system

After the perfusion, the activity distribution in the liver was examined by SPECT/CT imaging (Discovery NM/CT 670, GE Healthcare, United Kingdom) and the fused SPECT/CT images were analysed using Xeleris Workstation (GE Healthcare).

Lastly, detector B was used to estimate the activity concentration at 20 positions over the liver which were then compared with the activity concentration in biopsies sampled in the corresponding locations (Figure 6). The activity concentration estimated by detector B was calculated based on the measured count rate using data from the phantom measurements of organ thickness dependence as a calibration. The activity concentration in the biopsies were determined by measurements in a gamma counter (Wallac 1480 Wizard 3", Wallac

Oy, Finland). Then, 30 additional biopsies were sampled and measured to further investigate the homogeneity of ^{177}Lu-octreotate distribution.

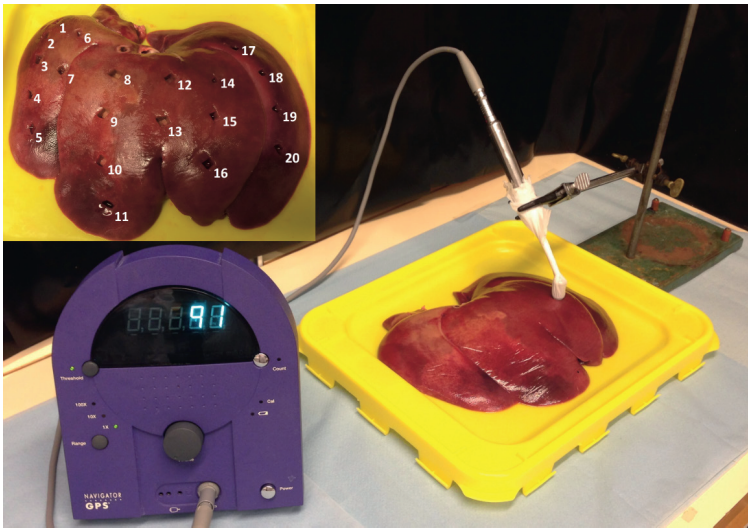

Figure 6. Detector B was used to estimate activity concentration at 20 positions after the IHP which were then compared with the activity concentration in corresponding biopsies

3.3 Combination therapy studies (Papers III-V)

Nude mice transplanted with patient-derived NETs were treated with different schedules of radiation therapy (as ^{177}Lu-octreotate or EBRT) and/or a drug. The drugs used were gemcitabine (Paper III), vandetanib and cabozantinib (Paper IV), and ganetespib (Paper V). All experiments were approved by the Ethical Committee on Animal Experiments in Gothenburg, Sweden.

3.3.1 NET animal models

Two NET animal models were used for the combination therapy studies, namely nude mice carrying GOT1 (Paper V) or GOT2 (Papers III-IV) tumours. GOT1 is an SI-NET cell line derived from a surgically removed liver metastasis of a patient [123]. The GOT2 cells were derived from a patient with sporadic MTC and transplanted to nude mice [124].

For the experiments, female BALB/c nude mice (Charles River Laboratories, Germany and Janvier Labs, France) were subcutaneously transplanted with small tumour samples of GOT1 or GOT2 (1x1x1 mm^3) under anaesthesia (Ketaminol® vet., Intervet AB, Sweden and Domitor® vet., Orion Pharma AB Animal Health, Sweden). Animals had free access to water and autoclaved food.

3.3.2 Radiation therapy

Radiation therapy was given as ^{177}Lu-octreotate (Papers III and V) or EBRT (Papers III and IV). ^{177}Lu-octreotate was administered by i.v. injection in the tail vein. EBRT was performed using a Varian linear accelerator with a 6 MV photon beam using a 30x30 mm^2 irradiation field (Varian Medical Systems, USA). The animals were anaesthetised and placed on their side on a tissue-equivalent polystyrene bed. Tissue-equivalent material was fitted around the tumour so that the centre of the tumour was at isocenter.

3.3.3 Drugs

Gemcitabine (Active Biochem LTD, China) was dissolved in saline solution and administered by intraperitoneal (i.p.) injection (Paper III). Vandetanib (Active Biochem LTD) was dissolved in a solution of PBS (Thermo Fisher Scientific, USA) and 1% polysorbate 80 (TWEEN® 80, Sigma-Aldrich, USA) and given by oral administration (Paper IV). Cabozantinib (Active Biochem LTD) was dissolved in sterile water and given by oral administration (Paper IV). Ganetespib (Selleckchem, Germany) was dissolved in a solution of sterile water, 5% DMSO, and 45% PEG and administered by i.v. injection in the tail vein (Paper V).

3.3.4 Treatment schedules and follow-up

Mice bearing GOT1 or GOT2 tumours were divided into groups of 5-12 mice per group and treated with different schedules of radiation therapy and/or a drug. The ^{177}Lu activity, absorbed dose and amount of drug were chosen to give a low to moderate effect as monotherapy to enable detection of any increased effects in the combination therapy groups. A detailed overview is given in Table 2.

Table 2. Overview of the treatment schedules used for the combination therapy studies (Papers III-V). Nude mice transplanted with patient-derived tissue from MTC (GOT2) or SI-NET (GOT1) were treated with ^{177}Lu-octreotate (^{177}Lu), external beam radiotherapy (EBRT), gemcitabine (Gem), vandetanib (Vand), cabozantinib (Cabo), and/or ganetespib (Gane). In some studies (Papers IV-V), the drug solvent was administered to the radiation therapy and control groups. Included are also the number of animals in each group (n), the follow-up time (T)

					Radiation therapy		Drug	
Paper	Model	Group	n	T (d)	Amount	Schedule	Amount	Schedule
III	GOT2	^{177}Lu	5	16	10 MBq	Single treatment	-	-
		Gem high	5	16	-	-	125 mg/kg[a]	Twice weekly
		^{177}Lu + Gem high	5	16	10 MBq	Single treatment	125 mg/kg[a]	Twice weekly
		EBRT	5	44	5 Gy	Single treatment	-	-
		Gem low	10	44	-	-	60 mg/kg	Twice weekly[b]
		EBRT + Gem low	6	58	5 Gy	Single treatment	60 mg/kg	Twice weekly[b]
		Control	12	30	-	-	-	-
IV	GOT2	EBRT	6	52	3 Gy	Single treatment	Solvent	Twice weekly
		Vand	5	52	-	-	100 mg/kg	Twice weekly
		EBRT + Vand	7	52	3 Gy	Single treatment	100 mg/kg	Twice weekly
		Control	8	31	-	-	Solvent	Twice weekly
		EBRT	5	49	3 Gy	Single treatment	Solvent	Twice weekly
		Cabo	8	49	-	-	50 mg/kg	Twice weekly
		EBRT + Cabo	5	49	3 Gy	Single treatment	50 mg/kg	Twice weekly
		Control	7	28	-	-	Solvent	Twice weekly
V	GOT1	^{177}Lu	5	14	15 MBq	Single treatment	Solvent	Single treatment
		Gane	5	14	-	-	50 mg/kg	Single treatment
		^{177}Lu + Gane	5	14	15 MBq	Single treatment	50 mg/kg	Single treatment
		Control	6	14	-	-	Solvent	Single treatment

[a]The amount was reduced to 60 mg/kg after three administrations. [b]Treatment was discontinued after five administrations.

After start of treatment, the length, width, and height of the tumours were measured twice weekly using digital callipers, and the tumour volume was calculated by assuming an ellipsoidal shape. At the end of each study, the mice were killed by cardiac puncture under anaesthesia (Pentobarbitalnatrium vet., Apotek Produktion & Laboratorier, Sweden). Before that, a mouse was killed if the tumour reached a volume corresponding to more than 10% of the body weight, if the body weight was reduced by more than 10%, or if the mouse showed any signs a poor general condition.

3.3.5 Internal dosimetry

The absorbed dose to tumours was calculated for the animals that received ^{177}Lu-octreotate (Papers III and V). The administered activity was determined by measuring the activity in each syringe before and after injection. The absorbed dose, D, was calculated using the Medical Internal Radiation Dose (MIRD) formalism [125]:

$$D = \frac{\tilde{A}\sum_i E_i Y_i \phi_i}{M}, \quad (2)$$

where $\tilde{A}$ is the time-integrated activity, the product E_iY_i is the energy emitted per decay, ϕ_i is the absorbed fraction, and M is the mass of the tumour. Only the contribution from electrons was considered. Therefore, $\sum E_iY_i$ was set to 147.9 keV and ϕ_i was set to 1 [65, 126]. $\tilde{A}$ was estimated from previously published data on biodistribution of ^{177}Lu-octreotate in nude mice carrying GOT1 or GOT2 tumours [127, 128].

3.3.6 Immunohistochemistry

Tumours were fixed in formalin, dehydrated, embedded in paraffin, sliced into sections, and stained with haematoxylin and eosin (H&E) for morphological examination. Some sections were stained with Masson's trichrome (MT) to analyse fibrosis (Paper III).

For immunohistochemical (IHC) analysis, tumour sections were placed on glass slides and treated with EnVision™ FLEX Target Retrieval Solution (high pH) using a PT-Link (Dako, Denmark). IHC staining was performed using an Autostainer Link with EnVision™ FLEX (Dako). The following primary antibodies were used: Ki67 (AB9260, Merck Millipore, USA), chromogranin A (ab68271, Abcam and EP1030Y, Abcam), synaptophysin (ab16659, Abcam and SP11, Abcam), calcitonin (A0576, Dako), serotonin (LS-B7118, LSBio, USA), pan-cytokeratin (AE1/AE3, Dako), SSTR2A (UMB-1, Abcam), and HSP90 (EPR3953, Abcam). Positive and negative controls were included in each run.

Tumour sections from animals treated with EBRT and/or gemcitabine stained for Ki67 and MT (Paper III) were digitalised and quantitatively analysed using an in-house developed MATLAB tool (R2017a, MathWorks, USA). By applying colour-thresholds, positively stained tissue could be segmented. Each section was divided into necrotic and viable tumour. Then, after excluding areas of background and artefacts, Ki67 staining was quantified in viable tumour, and MT staining (for collagen) was quantified for the entire tumour section.

3.3.7 Statistical analyses

To evaluate differences in tumour growth after start of treatment, group-wise mean relative tumour volumes (RTVs) were used for statistical analyses (Papers III-IV). RTV was individually defined as the tumour volume at a given time divided by the volume at treatment start. One-way ANOVA (GraphPad Prism 7.04, GraphPad Software, USA) was used to analyse overall differences between groups. Then, Student's t test with Bonferroni-Holm correction was used for group-to-group comparisons [129].

To analyse the potentially increased effect from combination therapy, the Bliss independence model was used to calculate a predicted additive effect based on the measured effects from monotherapy [130, 131]. Then, the measured effect in a combination therapy group was assumed to have been antagonistic, additive or synergistic if it was smaller than, equal to or larger than the predicted additive effect, respectively.

Note that for the results presented here, these above-mentioned statistical methods were applied also for the tumour-volume data from the combination therapy experiments involving ganetespib, while different statistical methods were used to analyse the interaction effect in the article (Paper V).

4 Results

4.1 Local administration (Papers I-II)

4.1.1 Phantom measurements (Paper I)

The two IGDs evaluated showed great differences in response (Figure 7). For detector A, the sensitivity and maximum measurable activity was 1200 cps/MBq and 6.1 MBq, respectively. The corresponding values for detector B was 500 cps/MBq and 28 MBq. Furthermore, the response was linear (within ±10%) for activities up to 1.3 and 12 MBq for detectors A and B, respectively.

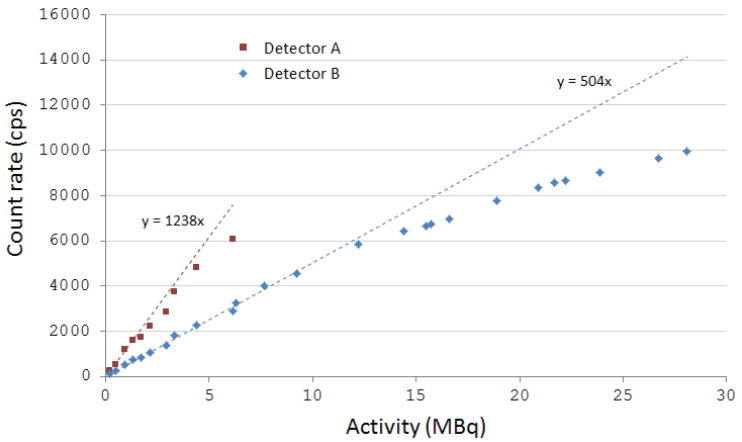

Figure 7. Detector response for point sources of different activities. Figure re-used from Paper I

Detector B had better spatial resolution than detector A (Figure 8). The largest relative difference in FWHM was 38% (at 20-mm depth). Furthermore, the response markedly decreased with increased depth of the line source for both detectors. At 10 mm depth, the response was 37% and 46% of the response at 0 mm for detector A and B, respectively.

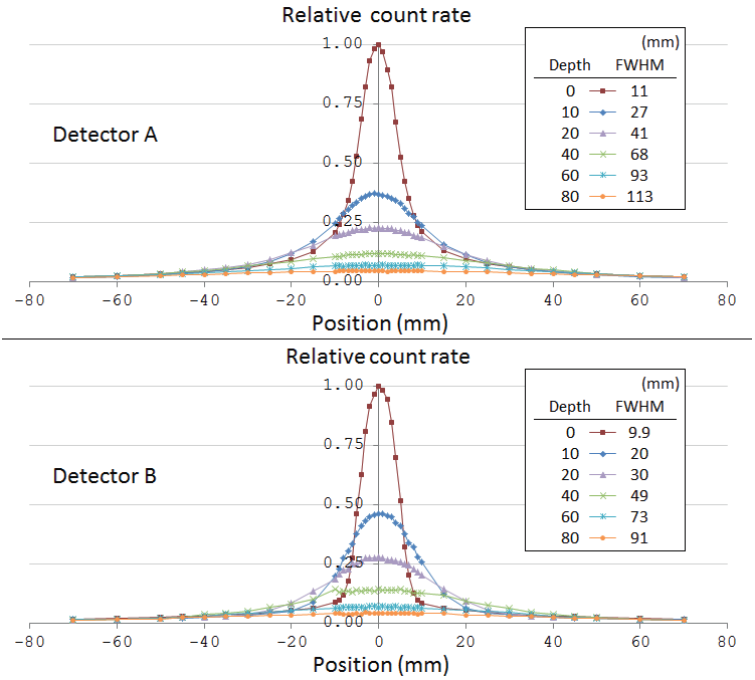

Figure 8. Detector response for the ^{177}Lu line source located at a depth of 0-80 mm. Spatial resolution is given as FWHM. Figure adapted with modification from Paper I

The evaluations of organs thickness dependence showed that the response increased with increasing thickness up to about 100 mm, after which a plateau was reached, for both detectors (Figure 9).

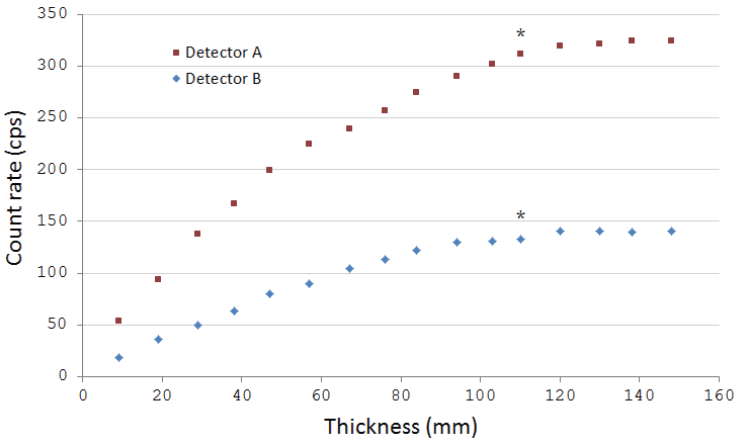

Figure 9. Organ thickness dependence of the detectors. The stars indicate the largest thickness where a statistically significant difference in count rate was found when compared with 148 mm. Figure re-used from Paper I

Regarding tumour detectability, detector B showed somewhat higher C_T/C_{Bgr} ratios (Figure 10). However, the situations where a statistically significant difference between C_T and C_{Bgr} was found were the same for both detectors.

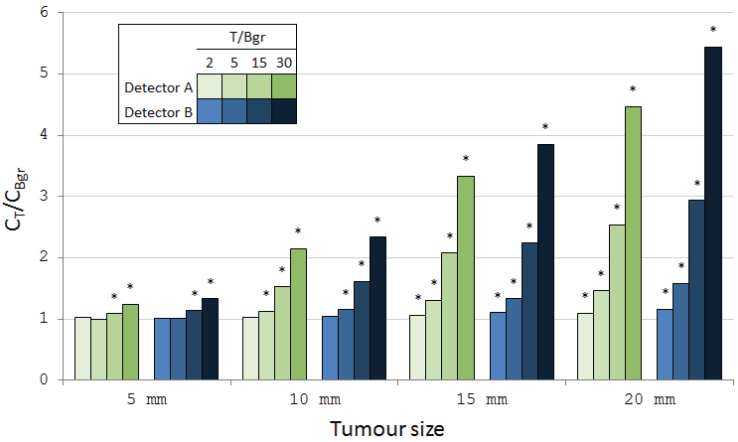

Figure 10. Tumour detectability given as the ratio between the count rate over a simulated tumour (C_T) and background (C_{Bgr}). The stars indicate that a statistically significant difference was found between C_T and C_{Bgr}. Figure re-used from Paper I

4.1.2 Simulation of the clinical situation (Paper II)

The radioactivity measurements during the IHP showed a fast increase of ^{177}Lu in the liver and a maximum was reached after about 10-15 minutes. When the rinsing was started, a fast decrease in count rate was seen, reaching a plateau after about 10-20 minutes. However, about 25% of the ^{177}Lu remained in the liver after the rinsing was finished. Furthermore, the SPECT/CT image (acquired after the perfusion and rinsing) revealed a relatively inhomogeneous distribution of ^{177}Lu in the liver with a coefficient of variation (CV=SD/mean) of 77% (Figure 11). An inhomogeneity was also seen in the 50 biopsies with a CV=36%.

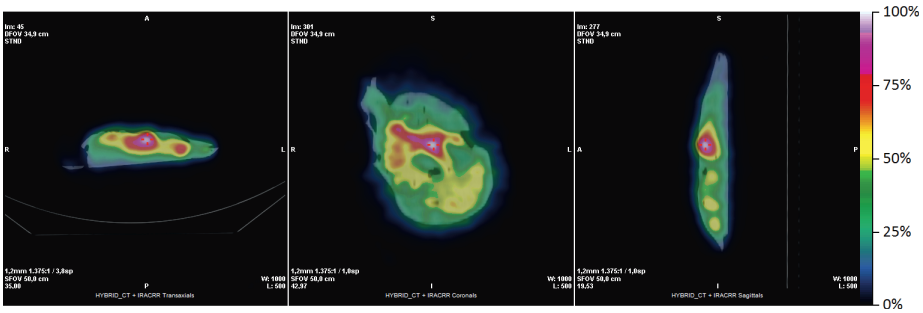

Figure 11. SPECT/CT image of the liver showing three different cross sections of the voxel with the highest value (indicated by the red cross)

After the IHP procedure and SPECT/CT imaging, the IGD (detector B) was used to estimate ^{177}Lu activity concentration (C_{IGD}) at several positions over the liver and the values were compared with biopsy measurements (C_B). Overall, the two methods showed a good agreement (Pearson's r=0.714 and p<0.001; Figure 12). The ratio between the activity concentrations measured with the two methods (C_{IGD}/C_B) ranged from 0.54 to 1.45 (mean=0.93, SEM=0.06).

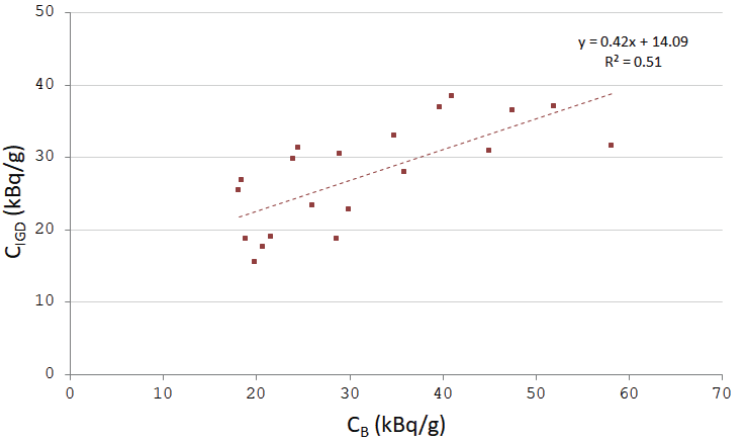

Figure 12. Activity concentration in the liver estimated by the IGD (C_{IGD}) vs. that in the biopsy (C_B) in the same position. R^2 is the coefficient of determination

None of the personal dosimeters worn by the staff during the IHP procedure gave any measureable radiation dose at readout. The highest ambient equivalent dose rates in the operating room were measured close to the liver. At the surface of the liver, the dose rate was 100 μSv/h, with corresponding values 10 and 4 μSv/h at 20 and 50-cm distance, respectively.

4.2 Combination therapy (Papers III-V)

4.2.1 Absorbed doses

Treatment with ^{177}Lu-octreotate resulted in absorbed doses of 0.13 Gy for GOT2 mice injected with 10 MBq (Paper III) and 2.7 Gy for GOT1 mice injected with 15 MBq (Paper V). As previously mentioned, the absorbed doses from EBRT were 5 Gy (Paper III) and 3 Gy (Paper IV).

4.2.2 Tumour growth

Given as monotherapy, all treatments resulted in clear effects on tumour volume compared with control even though suboptimal doses were deliberately chosen, except for ^{177}Lu-octreotate treatment in GOT2 mice (Paper III) which resulted in

a response similar to that of control (Figure 13). Generally, minimum RTVs were reached after about 10-20 days. For example, the smallest RTV for the animals that received monotherapy with vandetanib and cabozantinib was 0.98 ($RTV/RTV_{control}$=0.51, $p<0.001$) and 0.79 ($RTV/RTV_{control}$=0.44, $p<0.001$), respectively, at day 10 (Paper IV). Furthermore, EBRT monotherapy of GOT2 mice (Papers III-IV) and ^{177}Lu-octreotate monotherapy of GOT1 mice (Paper V), resulted in minimum RTVs of 0.57 ($RTV/RTV_{control}$=0.29, $p<0.001$, day 13) and 0.93 ($RTV/RTV_{control}$=0.61, $p=0.023$, day 10), respectively.

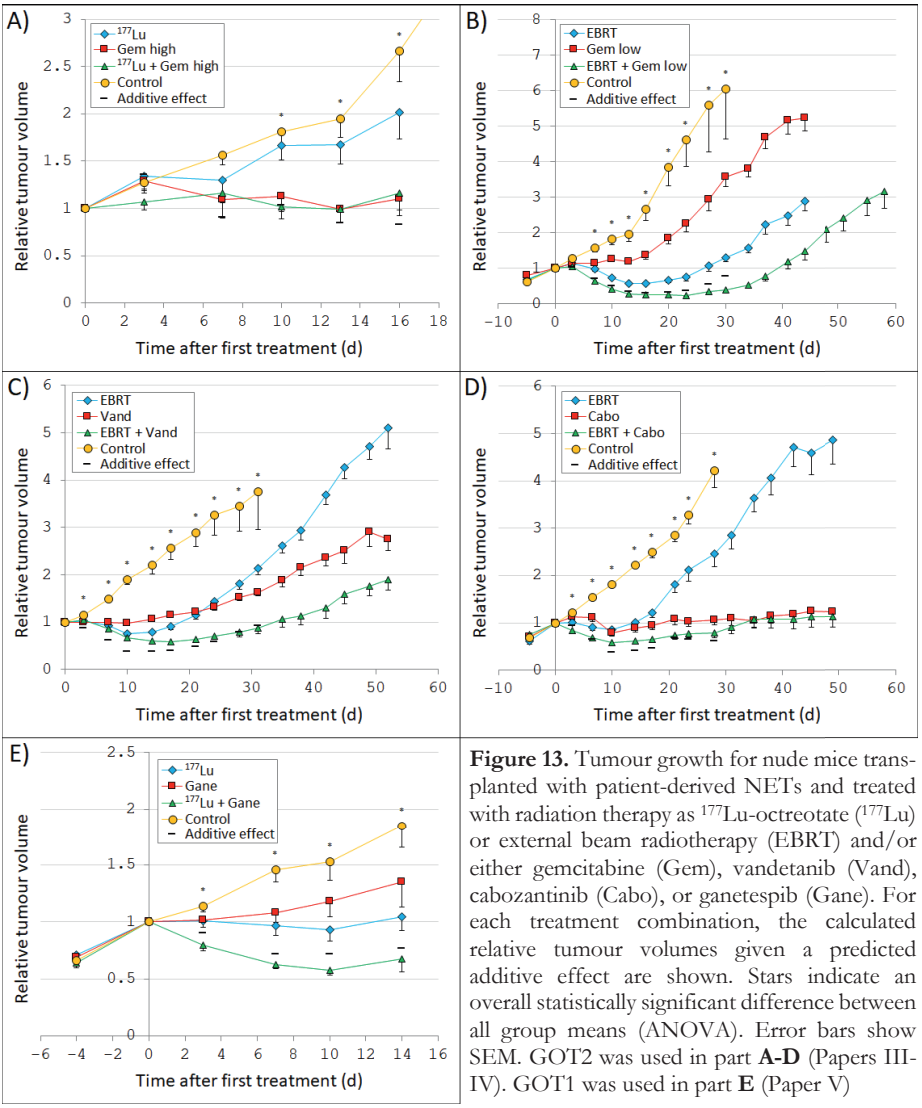

Figure 13. Tumour growth for nude mice transplanted with patient-derived NETs and treated with radiation therapy as ^{177}Lu-octreotate (^{177}Lu) or external beam radiotherapy (EBRT) and/or either gemcitabine (Gem), vandetanib (Vand), cabozantinib (Cabo), or ganetespib (Gane). For each treatment combination, the calculated relative tumour volumes given a predicted additive effect are shown. Stars indicate an overall statistically significant difference between all group means (ANOVA). Error bars show SEM. GOT2 was used in part **A-D** (Papers III-IV). GOT1 was used in part **E** (Paper V)

In all experiments, the largest reduction in tumour volume was seen for the animals that received combination therapy. In some experiments, the measured effect from combination therapy even appeared to be larger than the predicted additive effects, specifically in the experiments of EBRT plus gemcitabine (Paper III, Figure 13B) and ^{177}Lu-octreotate plus ganetespib (Paper V, Figure 13E). The measured effects of combining radiation therapy with TKIs vandetanib or cabozantinib appeared to be similar to the predicted additive effects (Paper IV, Figure 13C and D). The combination of ^{177}Lu-octreotate and gemcitabine resulted in similar effect as gemcitabine monotherapy (Paper III, Figure 13A).

4.2.3 Time to progression

Most treatments initially resulted in tumour volume reduction or tumour growth inhibition. However, regardless of given treatment, the tumours started to regrow after a certain time, even when treatment was continuously administered during the entire follow-up. Tumour progression was defined to occur when a tumour was larger than at start of treatment or when an animal was killed, and curves of progression-free survival in all experiments are shown in Figure 14. All treatments resulted in a prolonged time to progression compared with control (except for ^{177}Lu-octreotate monotherapy in GOT2 mice, Paper III). Tumour progression for the control animals was generally reached after about 0-10 days. The time to progression for the treated animals varied substantially with treatment from about 10 to 50 days, and in some cases, tumour progression had not been reached at the end of follow-up. Overall, combination therapy generally resulted in a longer time to progression than both monotherapy and control.

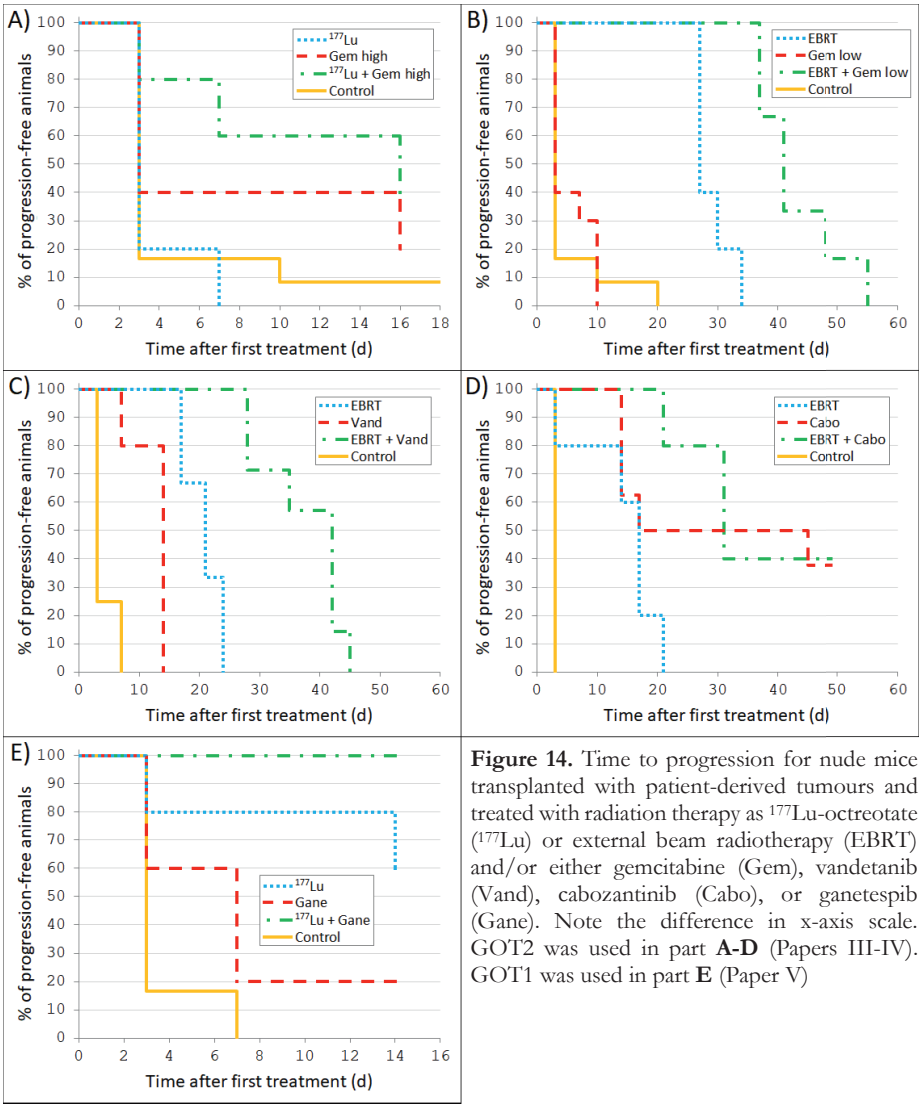

Figure 14. Time to progression for nude mice transplanted with patient-derived tumours and treated with radiation therapy as ^{177}Lu-octreotate (^{177}Lu) or external beam radiotherapy (EBRT) and/or either gemcitabine (Gem), vandetanib (Vand), cabozantinib (Cabo), or ganetespib (Gane). Note the difference in x-axis scale. GOT2 was used in part **A-D** (Papers III-IV). GOT1 was used in part **E** (Paper V)

4.2.4 Immunohistochemistry

The GOT1 and GOT2 tumours used in this study had maintained characteristics of NETs. All tumours stained for SI-NET or MTC markers showed a high and specific expression of all markers (chromogranin A, synaptophysin, calcitonin, serotonin, and pan-cytokeratin), verifying the origin of the GOT1 and GOT2 tumours (Figure 15). In addition, the GOT1 tumours also stained strongly for HSP90 and SSTR subtype 2.

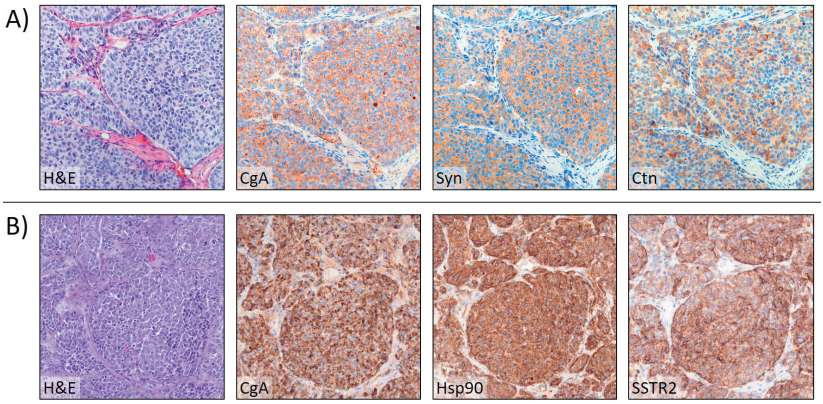

Figure 15. Morphology of two representative tumours from untreated control groups showing neuroendocrine differentiation with strong IHC staining for MTC and/or SI-NET markers chromogranin A (CgA), synaptophysin (Syn), and calcitonin (Ctn). **A)** GOT2 (Paper IV), and **B)** GOT1 (Paper V). The GOT1 tumours also stained strongly for HSP90 and SSTR subtype 2. Figure adapted with modification from Paper V

The quantification of Ki67 and MT staining in the sections of tumours harvested at the end of follow-up (day 30-58) after the experiments of EBRT in combination with gemcitabine (Paper III) showed overall a similar degree of staining in all tumours (Figure 16). The overall median was 64% and 3.0% for Ki67 and MT, respectively. However, several tumours that received treatment had a higher degree of MT-positive staining (of about 5-8%) than all untreated tumours which were similar to the overall median.

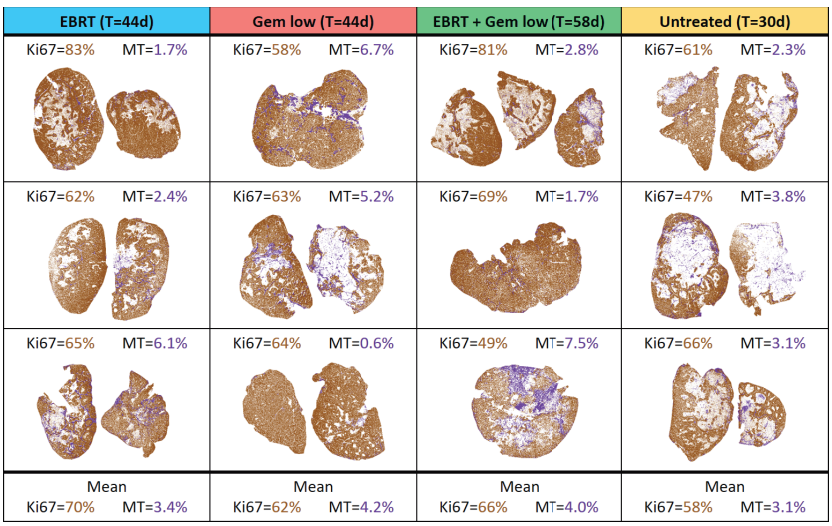

Figure 16. Quantitative results of Ki67 (brown) and MT (purple) staining analysed for the animals treated with 5 Gy external beam radiotherapy (EBRT) and/or 60 mg/kg gemcitabine (Gem low), and their corresponding untreated controls. T=follow-up time

5 Discussion

Radionuclide therapy with ^{177}Lu-octreotate is a promising treatment option for patients with metastatic NETs. However, because of the current standardised treatment protocol, few patients achieve complete response after ^{177}Lu-octreotate therapy. Several possible options for treatment optimisation exist. The main goal is to increase the effect on tumour tissue and/or to reduce side effects in healthy organs at risk. This could be achieved by investigating the optimal amount of peptide and activity per administration, optimal fractionation schedule, new radio-protecting or kidney-blocking agents, tolerance doses for healthy tissue, methods to increase SSTR expression, techniques for local administration, or combination therapy [66]. For example, tumour SSTR expression and uptake could be increased by pre-treatment with a small amount of ^{177}Lu-octreotate, a so-called priming administration [128]. There is also data showing that the amount of peptide and activity affects the uptake and biodistribution in both tumours and normal tissues [132, 133]. It is possible that the total amount of administered activity given according to the standardised treatment protocol can be increased [56, 134]. With increased knowledge, individual treatment planning could be performed, taking into account individual differences in biodistribution and radiation sensitivity of tumours and healthy organs. In this thesis, optimisation methods based on local administration and combination therapy were investigated.

5.1 Local administration (Papers I-II)

The purpose of a local administration is to increase the uptake of the radiopharmaceutical in a tissue of interest, *e.g.* a tumour, and to reduce the uptake in healthy organs at risk. Administration of ^{177}Lu-octreotate via IHP is a novel technique suggested for local treatment of liver metastases from NETs. Compared with a systemic administration, this technique should result in a substantially reduced uptake in tissues and organs outside the isolated liver circuit, based on knowledge from the clinically established IHP procedure, where melphalan is used to treat liver metastases from melanoma [72]. As previously mentioned, there are other techniques for local treatment of liver metastases from NETs, *e.g.* RE and intra-arterial PRRT [67, 68, 135]. However, since these local treatments are given with the systemic circulation intact, they differ substantially from the technique of ^{177}Lu-octreotate therapy during IHP, where the liver would be completely isolated during treatment.

One major drawback of local treatment of liver metastases is that it is only feasible for patients with metastatic spread confined to the liver. In addition, the primary

tumour must have been removed completely during surgery (something that is often possible). However, for patients that fulfil these criteria, the administration of ^{177}Lu-octreotate via IHP could be a very useful treatment option. Another limitation of this new technique is that the uptake of ^{177}Lu-octreotate in healthy liver tissue would not be reduced as it would for tissues and organs outside the isolated liver circuit. If this treatment should be used for patients, close attention must be given to the uptake and activity concentration in healthy liver tissue.

For systemic ^{177}Lu-octreotate therapy, the kidneys and the bone marrow are the main organs at risk, and the tolerance doses of these organs have therefore received far more attention than that of the liver. Data from EBRT and RE with ^{90}Y microspheres suggest that the tolerance dose of the liver strongly depends on the volume irradiated [136, 137]. In a review summarising data from EBRT, absorbed doses to the liver that resulted in less than 5% of patients developing with severe side effects were 40-80, 30-50, and 25-35 Gy if 1/3, 2/3, and the entire liver volume was irradiated, respectively [137]. These values are similar to those presented in the 1991 landmark article on tolerance doses from EBRT by Emami et al. [138]. On the other hand, clinical studies on ^{90}Y-RE suggest that absorbed doses to the whole liver of up to 100 Gy, or even more, can be safely given to patients [139-141]. Furthermore, for systemic ^{177}Lu-octreotate therapy, liver toxicity is extremely rare, and for this treatment, the mean absorbed dose to the liver is about 0.2-0.6 Gy/GBq, resulting in a total absorbed dose of about 6-30 Gy after 4-6 treatment cycles of 7.4 GBq [43, 48, 89, 142-144]. Altogether, the tolerance dose of the liver after ^{177}Lu-octreotate therapy given via IHP might be substantially higher than the values of about 30 Gy suggested for EBRT.

To be able to estimate the absorbed dose to healthy liver and NET liver metastases, information about absorbed fractions, organ masses, and biokinetics, both during and after IHP, is needed [125]. The results from the clinical simulation (Paper II) suggest that a certain amount of ^{177}Lu-octreotate will remain in the liver after the IHP and rinsing is finished. The activity concentration in liver and metastases after IHP could be determined using a gamma camera at different times after treatment (*e.g.* day 7 and 14). The biological half-life of ^{177}Lu-octreotate in liver tissue should be about 2-4 days [145-147]. There are several possible explanations to why a certain amount (about 25%) of ^{177}Lu-octreotate remained in the liver after the IHP simulation. Since neither hepatocytes nor hepatic stellate cells express SSTRs, one explanation could be difficulties in achieving a sufficient rinsing in all parts of the liver [148]. This would also explain the inhomogeneous activity distribution seen in the SPECT/CT images. It is also possible that part of the ^{177}Lu-octreotate had bound to SSTRs expressed by phagocytic Kupffer cells, hepatic lymphocytes, or by cells in the bile ducts [148, 149].

Determination of activity concentration also during IHP is important for estimations of absorbed doses. It should be possible to determine the activity concentration in vivo with satisfactory accuracy using an IGD if it is handled correctly and if certain factors are taken into account. The phantom measurements (Paper I) revealed dead-time effects at high activities for both IGDs evaluated that affected their response linearity and lead to a maximum measureable activity. In a therapeutic situation, high amounts of activity will be involved. Therefore, adding extra collimation to reduce the sensitivity could be beneficial to avoid reaching the maximum measureable activity. Extra collimation would also increase the spatial resolution. Furthermore, an organ thickness dependence was seen for both IGDs. This thickness dependence can be corrected for if the response curve is known. Therefore, it is important to calibrate IGDs by phantom measurements to be able to translate a measured count rate into an activity concentration. When using such a calibration, it is important to account for potential high-uptake regions at deeper locations. Lastly, since a relatively inhomogeneous uptake in healthy liver tissue was obtained after the IHP simulation, measurements at several positions over the liver might be needed to be able to correctly estimate the mean absorbed dose in a clinical situation. Based on the activity concentration values determined by an IGD (detector B) compared with those in the corresponding biopsies (C_{IGD}/C_B values), the uncertainty in an IGD-determined activity concentration at a given position over the liver is about ±50%. The total uncertainty in a calculated mean absorbed dose to the liver is estimated to be about ±60% (assuming independency between the individual uncertainties) [150]. However, if an inhomogeneous activity distribution is obtained also in a clinical situation, certain regions of the liver could receive higher doses than the calculated mean absorbed dose. The uncertainty in determining the activity concentration in a given tumour should be much lower than for healthy liver tissue, especially if the tumour is superficial and its size is similar to the field-of-view (FOV) of the IGD.

The radiation exposure of staff during an IHP procedure, that would involve relatively high amounts of ^{177}Lu-octreotate, should be possible to keep below regulatory limits. During the IHP simulation, all staff members could be positioned at a distance and often behind protective screens throughout most of the procedure, and consequently, no personal radiation doses were recorded. The same is possible in a clinical situation but one major difference exists. In a clinical situation, the surgeon must remove all tubes and close the surgical field. This would lead to a certain degree of radiation exposure, but based on the environmental exposure measurements during the IHP simulation, the total personal dose received after one procedure should be around 25 μSv. In Sweden, the annual dose limit for staff is 20 mSv, a limit that would be reached after about 800 procedures [151].

There are limitations of the IHP simulation and the IGD evaluations. Firstly, the IHP simulation was performed ex vivo. The ex vivo setting was chosen because even a very low contamination of the pig would result in logistic problems when handling the carcass after the experiment. However, based on previous knowledge and experience from the standard IHP procedure with melphalan, the ex vivo perfusion should not have affected the results obtained [69]. Another limitation was that the simulation was carried out as a terminal experiment in which the systemic circulation was not re-established after the perfusion and rinsing were finished. It would be valuable to have included this part in the simulation to investigate potential leakage of ^{177}Lu-octreotate to other organs outside the isolated circulation. Since the effect of rinsing on the decrease in ^{177}Lu activity concentration appeared to wear off after about 10-20 minutes, re-establishing the systemic circulation should not have led to any substantial leakage to other organs. However, this must be closely monitored if the technique of administering ^{177}Lu-octreotate via IHP is used clinically. A third limitation is that the results of the IHP simulation are based on an experiment including only one pig. The simulation could be repeated to investigate if similar uptake and distribution of ^{177}Lu-octreotate during and after IHP would be obtained. Lastly, the count rate over the liver (representing the activity concentration) during the IHP and rinsing was measured at a fixed position using the IGD. The main focus of this measurement was on biokinetics and the fixed position was used to avoid uncertainties due to positioning. However, given the inhomogeneity revealed by the SPECT images, and the narrow FOV of the IGD, measurements at several positions or the use of another detector could have provided valuable information during the IHP and rinsing.

5.2 Combination therapy (Papers III-V)

Combination treatment is another approach for optimisation of ^{177}Lu-octreotate therapy investigated in this thesis. The main goal of combination therapy is to achieve an increased anti-tumour effect compared with either treatment alone. Ideally, a synergistic effect would be achieved but combination therapy can be useful also at additive levels, especially if two drugs with different toxicity profiles are used.

When selecting drugs to use in combination with irradiation for treatment of NETs, many potential options exist. The drugs used for the combination therapy experiments (Papers III-V) were chosen for different reasons. Gemcitabine was chosen mainly because of the well-documented radiosensitising effect in other cancer types [96]. In addition, previous studies have shown that SSTR expression could be upregulated by gemcitabine [152, 153]. TKIs vandetanib and

cabozantinib were chosen because of their promising clinical results and because of the approval of these drugs for systemic treatment of metastatic MTC [24, 25]. Ganetespib was selected based on the results of a large-scale drug screening performed as a part of Paper V. Two cell lines derived from SI-NETs (GOT1 and P-STS) were screened using a drug library consisting of 1224 inhibitors alone or in combination with EBRT. The screening revealed that HSP90 inhibitors could potentiate the anti-tumour effect from radiation in SI-NETs. In addition, ganetespib has shown promising radiosensitising effects in other cancer types and is one of the most clinically successful HSP90 inhibitors [117-120, 154].

The radiation-drug-combinations evaluated within the work of this thesis revealed increased anti-tumour effects that appeared to be either additive or synergistic depending on the drug used. Gemcitabine appeared to synergistically potentiate the effect of radiation therapy on patient-derived MTC tumours in nude mice (Paper III). The mechanism behind a potential synergistic effect could be related to alterations in cellular response to radiation-induced DNA damage caused by gemcitabine. After entering the cell, gemcitabine acts as a nucleoside analogue of cytidine and its active metabolites are incorporated into the DNA which can lead to inhibition of DNA damage repair [96]. In addition, gemcitabine interferes with the enzyme ribonucleotide reductase involved in DNA synthesis and repair. Another drug that appeared to synergistically potentiate radiation therapy is HSP90 inhibitor ganetespib (Paper V). HSP90 regulates many client proteins that are involved in proliferation, survival, oncogenesis and cancer progression [154]. Therefore, cancer cells rely on a high expression of HSP90 and are sensitive to HSP90 inhibitors. Inhibition of HSP90 has been shown to predominantly target components of the cellular DNA damage response [155]. The mechanisms behind a synergistic interaction between radiation therapy and inhibition of HSP90 have been suggested to be related to downregulation of DNA repair and cell growth oncoproteins as well as cell cycle checkpoint activation [156-158]. Lastly, combination therapy using irradiation and TKIs vandetanib/cabozantinib resulted in increased anti-tumour effects (Paper IV). These effects appeared to be additive, rather than synergistic, but the results still provide a useful option for optimisation of ^{177}Lu-octreotate therapy, especially since the toxicity profiles for vandetanib/cabozantinib and ^{177}Lu-octreotate are somewhat different. The main side effects associated with vandetanib and cabozantinib are related to the gastrointestinal system [24, 25], while the main side effects for ^{177}Lu-octreotate therapy are haematological toxicity (usually reversible) and late renal toxicity [134, 159]. In addition, both TKI treatment and ^{177}Lu-octreotate therapy are already in clinical use for patients with MTC.

In some of the combination therapy experiments included in this thesis, EBRT was used instead of ^{177}Lu-octreotate. Specifically, EBRT was used for GOT2

tumours to obtain an absorbed dose sufficiently high to result in the desired tumour-volume reduction. The absorbed dose from EBRT was 3 or 5 Gy. ^{177}Lu-octreotate treatment of GOT1 tumours resulted in a similar absorbed dose of 2.7 Gy, while the absorbed dose for GOT2 tumours after injection of ^{177}Lu-otreotate was much lower – only 0.13 Gy. Both EBRT of GOT2 tumours and ^{177}Lu-octreotate treatment of GOT1 tumours resulted in clear reductions in tumour volume. It is likely that similar effects would have been seen also for ^{177}Lu-octreotate treatment of GOT2 if a higher absorbed dose would have been achieved. However, there is a lack of MTC animal models with a sufficiently high uptake of ^{177}Lu-octreotate [127]. Therefore, EBRT was used for GOT2 tumours to be able to investigate potential interaction effects of combination therapy involving radiation on MTC, and to demonstrate that MTC is sensitive to irradiation. Clinically, there is a large variation in SSTR expression between patients with MTC but many patients demonstrate a much higher tumour uptake than available MTC animal models with tumour-to-blood activity concentration ratios of up to 350, compared with about 25-50 for GOT2 tumours [121, 127, 160]. Furthermore, ^{177}Lu-octreoate has been used to treat MTC in several clinical studies [161-166]. The treatment outcome has varied between studies but, generally, ^{177}Lu-octreotate has proven to be a safe and effective treatment with response rates of about 40-70%. However, using one of the combination therapy strategies investigated here, the treatment outcome could be improved.

Two different NET animal models were used for the combination therapy experiments – nude mice carrying GOT1 (SI-NET) or GOT2 (MTC) tumours [123, 124]. These animal models provide valuable possibilities to study combination therapy strategies for NETs. There are other animal models available but the options are limited [66]. The following cell lines are all derived from human NETs or tumours with NET features and can be transplanted to nude mice in order to study different treatment effects in vivo. TT is an SSTR-expressing MTC cell line [167]. For example, vandetanib has shown clear anti-tumour effects by targeting RET in an animal model carrying TT tumours [168]. KRJ-I is a cell line established from an SI-NET [169]. However, this cell line has recently been shown to not display a neuroendocrine phenotype [170]. BON is a pancreatic NET cell line established from a lymph node metastasis [171]. IMR-32, CLB-BAR and CLB-GEMO are three SSTR-expressing neuroblastoma cell lines that have shown a high uptake of ^{177}Lu-octreotate in vivo [172]. There are also two lung cancer cell lines available, small cell lung cancer cell line NCI-H69 and bronchial NET cell line NCI-H727, and ^{177}Lu-octreotate therapy has been successfully used in animals carrying tumours from these cell lines [173-175].

Clinically, the most commonly used combination therapies involving PRRT are ^{177}Lu-octreotate in combination with capecitabine and/or temozolomide [88-91].

Many other drugs are being evaluated in preclinical studies as new and interesting candidates for combination therapy with ^{177}Lu-octreotate, *e.g.*, inhibitors of poly [ADP-ribose] polymerase 1 (PARP-1), nicotinamide phosphoribosyltransferase (NAMPT), HSP90, or Hedgehog. Olaparib is a PARP-1 inhibitor that has been shown to potentiate the anti-tumour effect of ^{177}Lu-octreotate in vitro (human osteosarcoma U2OS cells and rat pancreatic CA20948 cells) and ex vivo (patient-derived pancreatic NET tissue) by modulation of the DNA damage response leading to an increased number of double strand breaks [176]. GMX1778 is a NAMPT inhibitor (closely related to PARP-1) that increased the anti-tumour effect of ^{177}Lu-octreotate treatment in a study on nude mice carrying GOT1 tumours, both in regard to tumour-volume reduction and the duration of the effect [177]. Olanespib is a HSP90 inhibitor that displayed synergistic effects in combination with ^{177}Lu-octreotate in a 3D tumour spheroid model of NET cell lines [178]. The radiosensitising effect of this combination was also confirmed in vivo with low toxicity [179]. Sonidegib is a Hedgehog inhibitor that has been used in combination with ^{177}Lu-octreotate to treat nude mice carrying GOT1 tumours [180]. Combination treatment lead to profound reduction in tumour volume and a prolonged time to progression. Additionally, gene expression analysis revealed several cancer-related signalling pathways that were affected by the combination therapy indicating a functional interaction between ^{177}Lu-octreotate and sonidegib. The combination of ^{177}Lu-octreotate and everolimus (inhibitor of mammalian target of rapamycin, mTOR) is an approach that has shown less promising results. In preclinical in vivo studies on animals carrying human small cell lung cancer NCI-H69 tumours or rat pancreatic AR42J or CA20948 tumours, combination treatment resulted in anti-tumour effects less than or similar to the effects from ^{177}Lu-octreotate alone [181, 182]. Interestingly, combination treatment instead promoted formation of metastases, an effect that was not seen in control or ^{177}Lu-octreotate-treated animals [181]. Everolimus plus ^{177}Lu-octreotate therapy has also been evaluated for NETs in a clinical phase I study and many patients required dose reduction or treatment cessation [94].

There are limitations of the combination therapy studies included in this thesis. Firstly, the treatment groups within each experiment did not contain the same number of animals, and in some cases, the number of animals per group was relatively low. This is a result of the fact that the animal models used are practically difficult to work with. For example, the tumour take-rate and growth after transplantation is very unpredictable. It is difficult to plan experiments in full detail regarding, *e.g.*, number of mice per group, age of the mice, time between transplantation and start of treatment, tumour size at treatment start, or follow-up time. In order to keep such factors as similar as possible between treatment groups, each experiment were carried out in several smaller parts. Another limitation was that the dose-response for each monotherapy was not closely

evaluated. Even if the absorbed doses and administered amounts were chosen to result in moderate effects, a certain variation in the effect of monotherapy was seen between experiments. Information about an appropriate dose/amount was available from similar experiments for some treatments, but in some cases, a small pilot experiment was performed. Since different doses/amounts were used for different treatments, and since maximum therapeutic effects were most likely not reached, it is difficult to compare the treatments regarding which treatment had the largest anti-tumour effect. However, the deliberate use of suboptimal doses/amounts enabled analysis of the interaction effects when two treatments were combined, which was the main aim of these experiments. Higher doses/amounts would probably have led to larger therapeutic effects with possible cure in some animals.

6 Conclusions

Radionuclide therapy with ^{177}Lu-octreotate has proven to be a very successful treatment option for patients with neuroendocrine tumours since its introduction. However, complete response is rare and there is room for optimisation. In this work, two strategies for optimisation of ^{177}Lu-octreotate therapy were explored: 1) local drug administration (Papers I-II), and 2) combination therapy (Papers III-V). The main conclusions are summarised as follows.

Acceptable results were obtained for both intraoperative gamma detectors evaluated by phantom measurements (Paper I). The evaluations demonstrated factors that have to be corrected for, *e.g.* organ thickness and dead-time effects. Nevertheless, intraoperative gamma detector measurements could be used to determine ^{177}Lu activity concentration in vivo with reasonable accuracy.

It can be possible to treat patients with liver metastases from neuroendocrine tumours by administering ^{177}Lu-octreotate via isolated hepatic perfusion (Paper II). However, to account for a potentially inhomogeneous distribution of ^{177}Lu-octreotate in healthy liver tissue, intraoperative gamma detector measurements may need to be performed at several positions over the liver to more correctly determine the activity concentration.

Gemcitabine increased the anti-tumour effect of radiation therapy in mice carrying patient-derived medullary thyroid cancer, GOT2 (Paper III). The interaction between the effects of respective monotherapy appeared to act in a synergistic manner.

Combination therapy using tyrosine kinase inhibitors vandetanib or cabozantinib and external beam radiotherapy resulted in increased therapeutic effects in mice carrying patient-derived medullary thyroid cancer, GOT2 (Paper IV). It is likely that similar combinatorial effects would be achieved if ^{177}Lu-octreotate is used instead of external beam radiotherapy.

Ganetespib increased the anti-tumour effect of ^{177}Lu-octreotate treatment in mice carrying patient-derived small-intestine neuroendocrine tumours, GOT1 (Paper V). The interaction between the effects of respective monotherapy appeared to act in a synergistic manner.

7 Future perspectives

In this thesis, different aspects of ^{177}Lu-octreotate therapy optimisation were investigated by experimental studies based on local administration or combination therapy. The results of these studies demonstrated interesting options for optimisation that should be further evaluated in future studies.

The combined use of ^{177}Lu-octreotate therapy and IHP was successfully simulated ex vivo using a pig model. Future studies should evaluate this new treatment technique in patients with metastatic spread of NETs confined to the liver. The process of acquiring ethical approval for conducting such studies is currently on-going. When first implementing this treatment clinically, close attention must be given to potential side effects in healthy liver tissue. Measurements of the activity concentration during and after the IHP procedure is crucial to estimate the absorbed dose to healthy liver in order to determine which amount of ^{177}Lu-octreotate that can be safely administered to patients. It will also be important to monitor potential leakage to organs outside the isolated circuit, especially after the systemic circulation has been re-established.

Several drugs were demonstrated to result in favourable anti-tumour effects when combined with radiation therapy in nude mice carrying patient-derived NETs. These drugs could be administered in combination with ^{177}Lu-octreotate in order to treat patients with metastatic NETs. Before proceeding to clinical use, further preclinical studies should investigate potential short-term and long-term side effects of these treatment combinations in healthy tissues. It will also be important to investigate the optimal administration schedule for each of these treatment combinations in preclinical studies. Important parameters of an optimal administration schedule include administered amount, number of fractions (a single or several administrations), time between fractions, order in which the treatments should be administered, and time between start of respective treatment. The optimal administration schedule should be chosen to maximise the anti-tumour effect while still keeping side effects at an acceptable level. Following these preclinical investigations, the most promising combination treatment protocols should be evaluated in patients with NETs.

Lastly, ^{177}Lu-octreotate therapy could be further optimised by combining the two strategies investigated. It would be very interesting to investigate the potential of administering ^{177}Lu-octreotate in combination with another drug by IHP to treat patient with liver metastases from NETs.

Acknowledgements

Many people have helped me in so many ways during my years as a PhD student. Without these, this work would not have been possible. I would like to express my gratitude to all of you!

I would especially like to thank my supervisor Eva Forssell-Aronsson for your great knowledge, and for your support, guidance and constructive criticism. Our meetings always generate new energy and motivation to keep me going. Thank you for giving me the opportunity to explore the world of academic research. I would also like to thank my co-supervisor Khalil Helou for being a great example of a scientific researcher.

Another mentor during my PhD years has been Roger Olofsson Bagge. Thank you for introducing me to the very interesting technique of isolated hepatic perfusion and for our unique collaboration regarding this technique. It is always so captivating and very interesting to listen to you talk about science and research. And thank you Ola Nilsson, for teaching me so much about histology and biology in research.

I would also like to thank all my other co-authors for excellent collaborations. A special thanks to Ingun, Johan, and Tobias. I really enjoyed having you so close to me during this time. You made everything so much easier.

Next, I want to thank all past and present members of the Forssell-Aronsson Lab, for the time we shared in the research group both at home ground and at our research-related trips. Thank you Ann, Arman, Britta, Charlotte, Emil, Emman, Eva, Ingun, Johan, Johanna, Lilian, Malin, Maria, Micke, Mikael, Nils, and Sofia.

I also want to thank everyone at the Department of Radiation Physics, the Department of Medical Physics and Biomedical Engineering, and the Sahlgrenska Cancer Center, especially all members of Doktorandgruppen.

Last, but absolutely not least, I want to thank my friends and my family for always being there for me. Johanna, you really are my special someone, and I'm so lucky to have met you. I love you! Also, thank you for completing this thesis by creating the beautiful cover illustration.

This work was supported by grants from the Swedish Research Council (grant no. 21073), the Swedish Cancer Society (grant no. 3427), BioCARE – a National Strategic Research Program at the University of Gothenburg, the Swedish state under the agreement between the Swedish government and the county councils – the ALF-agreement (ALFGBG-725101/725031), the King Gustav V Jubilee Clinic Cancer Research Foundation, the Sahlgrenska University Hospital Research Funds, the Assar Gabrielsson Cancer Research Foundation, the Adlerbertska Research Foundation, the Herbert & Karin Jacobsson Foundation, the Knut and Alice Wallenberg Foundation, the Royal Society of Arts and Sciences in Gothenburg (KVVS), and the Wilhelm and Martina Lundgren Research Foundation.

References

1. Modlin IM, Lye KD, Kidd M. A 5-decade analysis of 13,715 carcinoid tumors. *Cancer. 2003;97(4):934-959*.
2. Gustafsson BI, Kidd M, Modlin IM. Neuroendocrine tumors of the diffuse neuroendocrine system. *Current Opinion in Oncology. 2008;20(1):1-12*.
3. Beaumont JL, Cella D, Phan AT, et al. Comparison of health-related quality of life in patients with neuroendocrine tumors with quality of life in the general US population. *Pancreas. 2012;41(3):461-466*.
4. Wängberg B, Nilsson O, Johanson V, et al. Somatostatin receptors in the diagnosis and therapy of neuroendocrine tumors. *The Oncologist. 1997;2(1):50-58*.
5. Reubi JC, Waser B. Concomitant expression of several peptide receptors in neuroendocrine tumours: molecular basis for in vivo multireceptor tumour targeting. *European Journal of Nuclear Medicine and Molecular Imaging. 2003;30(5):781-793*.
6. Yao JC, Hassan M, Phan A, et al. One hundred years after "carcinoid": epidemiology of and prognostic factors for neuroendocrine tumors in 35,825 cases in the United States. *Journal of Clinical Oncology. 2008;26(18):3063-3072*.
7. Hauso O, Gustafsson BI, Kidd M, et al. Neuroendocrine tumor epidemiology. *Cancer. 2008;113(10):2655-2664*.
8. Lawrence B, Gustafsson BI, Chan A, et al. The epidemiology of gastroenteropancreatic neuroendocrine tumors. *Endocrinology and Metabolism Clinics of North America. 2011;40(1):1-18*.
9. Kim MK, Warner RR, Roayaie S, et al. Revised staging classification improves outcome prediction for small intestinal neuroendocrine tumors. *Journal of Clinical Oncology. 2013;31(30):3776-3781*.
10. Wells Jr SA, Asa SL, Dralle H, et al. Revised American Thyroid Association guidelines for the management of medullary thyroid carcinoma: the American Thyroid Association Guidelines Task Force on medullary thyroid carcinoma. *Thyroid. 2015;25(6):567-610*.
11. Hofstra RM, Landsvater RM, Ceccherini I, et al. A mutation in the RET proto-oncogene associated with multiple endocrine neoplasia type 2B and sporadic medullary thyroid carcinoma. *Nature. 1994;367(6461):375-376*.
12. Pavel M, Costa F, Capdevila J, et al. ENETS consensus guidelines update for the management of distant metastatic disease of intestinal, pancreatic, bronchial neuroendocrine neoplasms (NEN) and NEN of unknown primary site. *Neuroendocrinology. 2016;103(2):172-185*.
13. Del Prete M, Fiore F, Modica R, et al. Hepatic arterial embolization in patients with neuroendocrine tumors. *Journal of Experimental & Clinical Cancer Research. 2014;33(1):43*.
14. Kress O, Wagner H-J, Wied M, et al. Transarterial chemoembolization of advanced liver metastases of neuroendocrine tumors–a retrospective single-center analysis. *Digestion. 2003;68(2-3):94-101*.
15. Cremonesi M, Chiesa C, Strigari L, et al. Radioembolization of hepatic lesions from a radiobiology and dosimetric perspective. *Frontiers in Oncology. 2014;4:210*.
16. Elf A-K, Andersson M, Henrikson O, et al. Radioembolization Versus Bland Embolization for Hepatic Metastases from Small Intestinal Neuroendocrine Tumors: Short-Term Results of a Randomized Clinical Trial. *World Journal of Surgery. 2018;42(2):506-513*.
17. Berber E, Flesher N, Siperstein AE. Laparoscopic radiofrequency ablation of neuroendocrine liver metastases. *World Journal of Surgery. 2002;26(8):985-990*.
18. Olausson M, Friman S, Herlenius G, et al. Orthotopic liver or multivisceral transplantation as treatment of metastatic neuroendocrine tumors. *Liver Transplantation. 2007;13(3):327-333*.

19. Rinke A, Müller H-H, Schade-Brittinger C, et al. Placebo-controlled, double-blind, prospective, randomized study on the effect of octreotide LAR in the control of tumor growth in patients with metastatic neuroendocrine midgut tumors: a report from the PROMID Study Group. *Journal of Clinical Oncology. 2009;27(28):4656-4663*.
20. Caplin ME, Pavel M, Ćwikła JB, et al. Lanreotide in metastatic enteropancreatic neuroendocrine tumors. *New England Journal of Medicine. 2014;371(3):224-233*.
21. Faiss S, Pape U-F, Böhmig M, et al. Prospective, randomized, multicenter trial on the antiproliferative effect of lanreotide, interferon alfa, and their combination for therapy of metastatic neuroendocrine gastroenteropancreatic tumors—the International Lanreotide and Interferon Alfa Study Group. *Journal of Clinical Oncology. 2003;21(14):2689-2696*.
22. Kulke MH, Hörsch D, Caplin ME, et al. Telotristat ethyl, a tryptophan hydroxylase inhibitor for the treatment of carcinoid syndrome. *Journal of Clinical Oncology. 2017;35(1):14-23*.
23. Yao JC, Shah MH, Ito T, et al. Everolimus for advanced pancreatic neuroendocrine tumors. *New England Journal of Medicine. 2011;364(6):514-523*.
24. Wells Jr SA, Robinson BG, Gagel RF, et al. Vandetanib in patients with locally advanced or metastatic medullary thyroid cancer: a randomized, double-blind phase III trial. *Journal of Clinical Oncology. 2012;30(2):134-141*.
25. Elisei R, Schlumberger MJ, Müller SP, et al. Cabozantinib in progressive medullary thyroid cancer. *Journal of Clinical Oncology. 2013;31(29):3639-3646*.
26. Faivre S, Niccoli P, Castellano D, et al. Sunitinib in pancreatic neuroendocrine tumors: updated progression-free survival and final overall survival from a phase III randomized study. *Annals of Oncology. 2017;28(2):339-343*.
27. Moertel CG, Lefkopoulo M, Lipsitz S, et al. Streptozocin–doxorubicin, streptozocin–fluorouracil, or chlorozotocin in the treatment of advanced islet-cell carcinoma. *New England Journal of Medicine. 1992;326(8):519-523*.
28. Strosberg JR, Fine RL, Choi J, et al. First-line chemotherapy with capecitabine and temozolomide in patients with metastatic pancreatic endocrine carcinomas. *Cancer. 2011;117(2):268-275*.
29. Kulke MH, Kim H, Clark JW, et al. A Phase II trial of gemcitabine for metastatic neuroendocrine tumors. *Cancer. 2004;101(5):934-939*.
30. Hung WW, Wang CS, Tsai KB, et al. Medullary thyroid carcinoma with poor differentiation and atypical radiographic pattern of metastasis. *Pathology International. 2009;59(9):660-663*.
31. Matuszczyk A, Petersenn S, Voigt W, et al. Chemotherapy with paclitaxel and gemcitabine in progressive medullary and thyroid carcinoma of the follicular epithelium. *Hormone and Metabolic Research. 2010;42(01):61-64*.
32. Proescher F. The intravenous injection of soluble radium salts in man. *Radium. 1913;1:9-10*.
33. Carlson S. A glance at the history of nuclear medicine. *Acta oncologica. 1995;34(8):1095-1102*.
34. Fischer M, Winterberg B, Friemann J, et al. Radioisotopic therapy of pheochromocytoma. *Nuc Compact: Compact News in Nuclear Medicine. 1983;14(4):172-176*.
35. Hoefnagel C, Den FHJ, Van AG, et al. Diagnosis and treatment of a carcinoid tumor using iodine-131 meta-iodobenzylguanidine. *Clinical Nuclear Medicine. 1986;11(3):150-152*.
36. Bakker W, Albert R, Bruns C, et al. [111In-DTPA-D-Phe1]-octreotide, a potential radiopharmaceutical for imaging of somatostatin receptor-positive tumors: synthesis, radiolabeling and in vitro validation. *Life Sciences. 1991;49(22):1583-1591*.
37. Forssell-Aronsson E, Fjälling M, Nilsson O, et al. Indium-111 activity concentration in tissue samples after intravenous injection of indium-111-DTPA-D-Phe-1-octreotide. *Journal of Nuclear Medicine. 1995;36(1):7-12*.

38. Reubi JC, Schär J-C, Waser B, et al. Affinity profiles for human somatostatin receptor subtypes SST1–SST5 of somatostatin radiotracers selected for scintigraphic and radiotherapeutic use. *European Journal of Nuclear Medicine. 2000;27(3):273-282*.
39. Krenning EP, Kooij PP, Bakker WeH, et al. Radiotherapy with a radiolabeled somatostatin analogue, [111In-DTPA-d-Phe1]-octreotide: A case history. *Annals of the New York Academy of Sciences. 1994;733(1):496-506*.
40. Fjälling M, Andersson P, Forssell-Aronsson E, et al. Systemic radionuclide therapy using indium-111-DTPA-D-Phe1-octreotide in midgut carcinoid syndrome. *Journal of Nuclear Medicine. 1996;37(9):1519-1521*.
41. Valkema R, de Jong M, Bakker WH, et al. Phase I study of peptide receptor radionuclide therapy with [111In-DTPA0]octreotide: the Rotterdam experience. *Seminars in Nuclear Medicine. 2002;32(2):110-122*.
42. Otte A, Herrmann R, Heppeler A, et al. Yttrium-90 DOTATOC: first clinical results. *European Journal of Nuclear Medicine. 1999;26(11):1439-1447*.
43. Kwekkeboom DJ, Bakker WH, Kooij PP, et al. [177Lu-DOTA0, Tyr3] octreotate: comparison with [111In-DTPA0] octreotide in patients. *European Journal of Nuclear Medicine. 2001;28(9):1319-1325*.
44. Kwekkeboom DJ, Bakker W, Kam B, et al. Treatment of patients with gastro-entero-pancreatic (GEP) tumours with the novel radiolabelled somatostatin analogue [177 Lu-DOTA 0, Tyr 3] octreotate. *European Journal of Nuclear Medicine and Molecular Imaging. 2003;30(3):417-422*.
45. Bodei L, Cremonesi M, Zoboli S, et al. Receptor-mediated radionuclide therapy with 90Y-DOTATOC in association with amino acid infusion: a phase I study. *European Journal of Nuclear Medicine and Molecular Imaging. 2003;30(2):207-216*.
46. Hicks RJ, Kwekkeboom DJ, Krenning E, et al. ENETS Consensus Guidelines for the Standards of Care in Neuroendocrine Neoplasia: Peptide Receptor Radionuclide Therapy with Radiolabelled Somatostatin Analogues. *Neuroendocrinology. 2017;105(3):295-309*.
47. Swärd C, Bernhardt P, Ahlman H, et al. [177Lu-DOTA0-Tyr3]-octreotate treatment in patients with disseminated gastroenteropancreatic neuroendocrine tumors: the value of measuring absorbed dose to the kidney. *World Journal of Surgery. 2010;34(6):1368-1372*.
48. Gupta SK, Singla S, Thakral P, et al. Dosimetric analyses of kidneys, liver, spleen, pituitary gland, and neuroendocrine tumors of patients treated with 177Lu-DOTATATE. *Clinical Nuclear Medicine. 2013;38(3):188-194*.
49. Ezziddin S, Khalaf F, Vanezi M, et al. Outcome of peptide receptor radionuclide therapy with 177Lu-octreotate in advanced grade 1/2 pancreatic neuroendocrine tumours. *European Journal of Nuclear Medicine and Molecular Imaging. 2014;41(5):925-933*.
50. Kong G, Thompson M, Collins M, et al. Assessment of predictors of response and long-term survival of patients with neuroendocrine tumour treated with peptide receptor chemoradionuclide therapy (PRCRT). *European Journal of Nuclear Medicine and Molecular Imaging. 2014;41(10):1831-1844*.
51. Bodei L, Kidd M, Paganelli G, et al. Long-term tolerability of PRRT in 807 patients with neuroendocrine tumours: the value and limitations of clinical factors. *European Journal of Nuclear Medicine and Molecular Imaging. 2015;42(1):5-19*.
52. Brabander T, Van der Zwan WA, Teunissen JJ, et al. Long-term efficacy, survival and safety of [177Lu-DOTA0, Tyr3] octreotate in patients with gastroenteropancreatic and bronchial neuroendocrine tumors. *Clinical Cancer Research. 2017;23(16):4617-4624*.
53. Brunner P, Jörg A-C, Glatz K, et al. The prognostic and predictive value of sstr 2-immunohistochemistry and sstr 2-targeted imaging in neuroendocrine tumors. *European Journal of Nuclear Medicine and Molecular Imaging. 2017;44(3):468-475*.

54. Pencharz D, Walker M, Yalchin M, et al. Early efficacy of and toxicity from lutetium-177-DOTATATE treatment in patients with progressive metastatic NET. *Nuclear Medicine Communications. 2017;38(7):593-600*.
55. Sansovini M, Severi S, Ianniello A, et al. Long-term follow-up and role of FDG PET in advanced pancreatic neuroendocrine patients treated with 177 Lu-DOTATATE. *European Journal of Nuclear Medicine and Molecular Imaging. 2017;44(3):490-499*.
56. Sundlöv A, Sjögreen-Gleisner K, Svensson J, et al. Individualised 177Lu-DOTATATE treatment of neuroendocrine tumours based on kidney dosimetry. *European Journal of Nuclear Medicine and Molecular Imaging. 2017;44(9):1480-1489*.
57. Garske-Román U, Sandström M, Baron KF, et al. Prospective observational study of 177Lu-DOTA-octreotate therapy in 200 patients with advanced metastasized neuroendocrine tumours (NETs): feasibility and impact of a dosimetry-guided study protocol on outcome and toxicity. *European Journal of Nuclear Medicine and Molecular Imaging. 2018;45(6):970-988*.
58. Kwekkeboom DJ, Teunissen JJ, Bakker WH, et al. Radiolabeled somatostatin analog [177Lu-DOTA0,Tyr3]octreotate in patients with endocrine gastroenteropancreatic tumors. *Journal of Clinical Oncology. 2005;23(12):2754-2762*.
59. Strosberg J, El-Haddad G, Wolin E, et al. Phase 3 trial of 177Lu-Dotatate for midgut neuroendocrine tumors. *New England Journal of Medicine. 2017;376(2):125-135*.
60. Strosberg J, Wolin E, Chasen B, et al. Health-related quality of life in patients with progressive midgut neuroendocrine tumors treated with 177Lu-dotatate in the phase III NETTER-1 trial. *Journal of Clinical Oncology. 2018;36(25):2578-2584*.
61. Uusijärvi H, Bernhardt P, Ericsson T, et al. Dosimetric characterization of radionuclides for systemic tumor therapy: influence of particle range, photon emission, and subcellular distribution. *Medical Physics. 2006;33(9):3260-3269*.
62. Krenning E, Kwekkeboom DJ, Bakker Wea, et al. Somatostatin receptor scintigraphy with [111In-DTPA-D-Phe1]- and [123I-Tyr3]-octreotide: the Rotterdam experience with more than 1000 patients. *European Journal of Nuclear Medicine. 1993;20(8):716-731*.
63. Gabriel M, Decristoforo C, Kendler D, et al. 68Ga-DOTA-Tyr3-octreotide PET in neuroendocrine tumors: comparison with somatostatin receptor scintigraphy and CT. *Journal of Nuclear Medicine. 2007;48(4):508-518*.
64. Srirajaskanthan R, Kayani I, Quigley AM, et al. The role of 68Ga-DOTATATE PET in patients with neuroendocrine tumors and negative or equivocal findings on 111In-DTPA-octreotide scintigraphy. *Journal of Nuclear Medicine. 2010;51(6):875-882*.
65. Eckerman K, Endo A. ICRP Publication 107. Nuclear decay data for dosimetric calculations. *Annals of the ICRP. 2008;38(3):7-96*.
66. Forssell-Aronsson E, Spetz J, Ahlman H. Radionuclide therapy via SSTR: future aspects from experimental animal studies. *Neuroendocrinology. 2013;97(1):86-98*.
67. McStay MK, Maudgil D, Williams M, et al. Large-volume liver metastases from neuroendocrine tumors: hepatic intraarterial 90Y-DOTA-lanreotide as effective palliative therapy. *Radiology. 2005;237(2):718-726*.
68. Singh A, Zhang J, Kulkarni H, et al. Survival and safety analysis of intra-arterial PRRT of SSTR-expressing tumors in over 50 patients: targeting NEN and beyond. *European Journal of Nuclear Medicine and Molecular Imaging. 2018;45(Suppl 1):S183-S184*.
69. Ben-Shabat I, Hansson C, Eilard MS, et al. Isolated hepatic perfusion as a treatment for liver metastases of uveal melanoma. *JoVE (Journal of Visualized Experiments). 2015(95):e52490-e52490*.
70. Bartlett DL, Libutti SK, Figg WD, et al. Isolated hepatic perfusion for unresectable hepatic metastases from colorectal cancer. *Surgery. 2001;129(2):176-187*.

71. Grover AC, Libutti SK, Pingpank JF, et al. Isolated hepatic perfusion for the treatment of patients with advanced liver metastases from pancreatic and gastrointestinal neuroendocrine neoplasms. *Surgery. 2004;136(6):1176-1182*.
72. Olofsson R, Cahlin C, All-Ericsson C, et al. Isolated hepatic perfusion for ocular melanoma metastasis: registry data suggests a survival benefit. *Annals of Surgical Oncology. 2014;21(2):466-472*.
73. Heller S, Zanzonico P. Nuclear probes and intraoperative gamma cameras. *Seminars in Nuclear Medicine. 2011;41(3):166-181*.
74. Ahlman H, Wängberg B, Tisell L, et al. Clinical efficacy of octreotide scintigraphy in patients with midgut carcinoid tumours and evaluation of intraoperative scintillation detection. *British Journal of Surgery. 1994;81(8):1144-1149*.
75. Benjegård SA, Forssell-Aronsson E, Wängberg B, et al. Intraoperative tumour detection using 111In-DTPA-D-Phe1-octreotide and a scintillation detector. *European Journal of Nuclear Medicine. 2001;28(10):1456-1462*.
76. Harvey WC, Lancaster JL. Technical and clinical characteristics of a surgical biopsy probe. *Journal of Nuclear Medicine. 1981;22(2):184-186*.
77. Curtet C, Vuillez J, Daniela G, et al. Feasibility study of radioimmunoguided surgery of colorectal carcinomas using indium-111 CEA-specific monoclonal antibody. *European Journal of Nuclear Medicine. 1990;17(6-8):299-304*.
78. Waddington WA, Davidson BR, Todd-Pokropek A, et al. Evaluation of a technique for the intraoperative detection of a radiolabelled monoclonal antibody against colorectal cancer. *European Journal of Nuclear Medicine. 1991;18(12):964-972*.
79. Benjegård SA, Sauret V, Bernhardt P, et al. Evaluation of three gamma detectors for intraoperative detection of tumors using 111In-labeled radiopharmaceuticals. *Journal of Nuclear Medicine. 1999;40(12):2094-2101*.
80. Britten AJ. A method to evaluate intra-operative gamma probes for sentinel lymph node localisation. *European Journal of Nuclear Medicine. 1999;26(2):76-83*.
81. Haigh PI, Glass EC, Essner R. Accuracy of gamma probes in localizing radioactivity: in-vitro assessment and clinical implications. *Cancer Biotherapy & Radiopharmaceuticals. 2000;15(6):561-569*.
82. Zamburlini M, Keymeulen K, Bemelmans M, et al. Comparison of sentinel gamma probes for 99mTc breast cancer surgery based on NEMA NU3-2004 standard. *Nuclear Medicine Communications. 2009;30(11):854-861*.
83. Johnsrud K, Skretting A, Naum AG, et al. Characterization of an asymmetric add-on collimator used with a hand-held gamma probe for radioguided surgery and sentinel node detection: a demonstration of an alternative collimation method. *Clinical Physiology and Functional Imaging. 2013;33(6):478-482*.
84. Eriksson D, Stigbrand T. Radiation-induced cell death mechanisms. *Tumor Biology. 2010;31(4):363-372*.
85. Wardman P. Chemical radiosensitizers for use in radiotherapy. *Clinical Oncology. 2007;19(6):397-417*.
86. Greco WR, Faessel H, Levasseur L. The search for cytotoxic synergy between anticancer agents: a case of Dorothy and the ruby slippers? *Journal of the National Cancer Institute. 1996;88(11):699-700*.
87. Palmer AC, Sorger PK. Combination cancer therapy can confer benefit via patient-to-patient variability without drug additivity or synergy. *Cell. 2017;171(7):1678-1691*.
88. van Essen M, Krenning EP, Kam BL, et al. Report on short-term side effects of treatments with 177Lu-octreotate in combination with capecitabine in seven patients with

gastroenteropancreatic neuroendocrine tumours. *European Journal of Nuclear Medicine and Molecular Imaging. 2008;35(4):743-748*.

89. Claringbold PG, Brayshaw PA, Price RA, et al. Phase II study of radiopeptide 177Lu-octreotate and capecitabine therapy of progressive disseminated neuroendocrine tumours. *European Journal of Nuclear Medicine and Molecular Imaging. 2011;38(2):302-311*.
90. Ballal S, Yadav MP, Damle NA, et al. Concomitant 177Lu-DOTATATE and capecitabine therapy in patients with advanced neuroendocrine tumors: a long-term-outcome, toxicity, survival, and quality-of-life study. *Clinical Nuclear Medicine. 2017;42(11):e457-e466*.
91. Claringbold PG, Turner JH. Pancreatic neuroendocrine tumor control: durable objective response to combination 177Lu-octreotate-capecitabine-temozolomide radiopeptide chemotherapy. *Neuroendocrinology. 2016;103(5):432-439*.
92. Thakral P, Sen I, Pant V, et al. Dosimetric analysis of patients with gastro entero pancreatic neuroendocrine tumors (NETs) treated with PRCRT (peptide receptor chemo radionuclide therapy) using Lu-177 DOTATATE and capecitabine/temozolomide (CAP/TEM). *The British Journal of Radiology. 2018;91(1091):20170172*.
93. Hubble D, Kong G, Michael M, et al. 177Lu-octreotate, alone or with radiosensitising chemotherapy, is safe in neuroendocrine tumour patients previously treated with high-activity 111In-octreotide. *European Journal of Nuclear Medicine and Molecular Imaging. 2010;37(10):1869-1875*.
94. Claringbold PG, Turner JH. Neuroendocrine tumor therapy with lutetium-177-octreotate and everolimus (NETTLE): a phase I study. *Cancer Biotherapy and Radiopharmaceuticals. 2015;30(6):261-269*.
95. Dadan J, Wolczyński S, Sawicki B, et al. Preliminary evaluation of influence of gemcitabine (Gemzar) on proliferation and neuroendocrine activity of human TT cell line: immunocytochemical investigations. *Folia Histochemica et Cytobiologica. 2001;39(2):187-188*.
96. Pauwels B, Korst AE, Lardon F, et al. Combined modality therapy of gemcitabine and radiation. *The Oncologist. 2005;10(1):34-51*.
97. de Sousa Cavalcante L, Monteiro G. Gemcitabine: metabolism and molecular mechanisms of action, sensitivity and chemoresistance in pancreatic cancer. *European Journal of Pharmacology. 2014;741:8-16*.
98. Shewach DS, Hahn TM, Chang E, et al. Metabolism of 2', 2'-difluoro-2'-deoxycytidine and radiation sensitization of human colon carcinoma cells. *Cancer Research. 1994;54(12):3218-3223*.
99. Lawrence TS, Chang EY, Hahn TM, et al. Radiosensitization of pancreatic cancer cells by 2', 2'-difluoro-2'-deoxycytidine. *International Journal of Radiation Oncology • Biology • Physics. 1996;34(4):867-872*.
100. Mason KA, Milas L, Hunter NR, et al. Maximizing therapeutic gain with gemcitabine and fractionated radiation. *International Journal of Radiation Oncology • Biology • Physics. 1999;44(5):1125-1135*.
101. Milas L, Fujii T, Hunter N, et al. Enhancement of tumor radioresponse in vivo by gemcitabine. *Cancer Research. 1999;59(1):107-114*.
102. Pauwels B, Korst AE, Pattyn GG, et al. Cell cycle effect of gemcitabine and its role in the radiosensitizing mechanism in vitro. *International Journal of Radiation Oncology • Biology • Physics. 2003;57(4):1075-1083*.
103. Blackstock AW, Bernard SA, Richards F, et al. Phase I trial of twice-weekly gemcitabine and concurrent radiation in patients with advanced pancreatic cancer. *Journal of Clinical Oncology. 1999;17(7):2208-2208*.

104. Eisbruch A, Shewach DS, Bradford CR, et al. Radiation concurrent with gemcitabine for locally advanced head and neck cancer: a phase I trial and intracellular drug incorporation study. *Journal of Clinical Oncology. 2001;19(3):792-799*.
105. McGinn CJ, Zalupski MM, Shureiqi I, et al. Phase I trial of radiation dose escalation with concurrent weekly full-dose gemcitabine in patients with advanced pancreatic cancer. *Journal of Clinical Oncology. 2001;19(22):4202-4208*.
106. Dueñas-González A, Zarbá JJ, Patel F, et al. Phase III, open-label, randomized study comparing concurrent gemcitabine plus cisplatin and radiation followed by adjuvant gemcitabine and cisplatin versus concurrent cisplatin and radiation in patients with stage IIB to IVA carcinoma of the cervix. *Journal of Clinical Oncology. 2011;29(13):1678-1685*.
107. Loehrer PJ, Feng Y, Cardenes H, et al. Gemcitabine alone versus gemcitabine plus radiotherapy in patients with locally advanced pancreatic cancer: an Eastern Cooperative Oncology Group trial. *Journal of Clinical Oncology. 2011;29(31):4105-4112*.
108. Capp C, Wajner SM, Siqueira DR, et al. Increased expression of vascular endothelial growth factor and its receptors, VEGFR-1 and VEGFR-2, in medullary thyroid carcinoma. *Thyroid. 2010;20(8):863-871*.
109. Ying W, Du Z, Sun L, et al. Ganetespib, a unique triazolone-containing Hsp90 inhibitor, exhibits potent antitumor activity and a superior safety profile for cancer therapy. *Molecular Cancer Therapeutics. 2012;11(2):475-484*.
110. Whitesell L, Lindquist SL. HSP90 and the chaperoning of cancer. *Nature Reviews Cancer. 2005;5(10):761-772*.
111. Yufu Y, Nishimura J, Nawata H. High constitutive expression of heat shock protein 90α in human acute leukemia cells. *Leukemia Research. 1992;16(6-7):597-605*.
112. Pick E, Kluger Y, Giltnane JM, et al. High HSP90 expression is associated with decreased survival in breast cancer. *Cancer Research. 2007;67(7):2932-2937*.
113. Goldman JW, Raju RN, Gordon GA, et al. A first in human, safety, pharmacokinetics, and clinical activity phase I study of once weekly administration of the Hsp90 inhibitor ganetespib (STA-9090) in patients with solid malignancies. *BMC Cancer. 2013;13(1):152*.
114. Socinski MA, Goldman J, El-Hariry I, et al. A multicenter phase II study of ganetespib monotherapy in patients with genotypically defined advanced non–small cell lung cancer. *Clinical Cancer Research. 2013;19(11):3068-3077*.
115. Ramalingam S, Goss G, Rosell R, et al. A randomized phase II study of ganetespib, a heat shock protein 90 inhibitor, in combination with docetaxel in second-line therapy of advanced non-small cell lung cancer (GALAXY-1). *Annals of Oncology. 2015;26(8):1741-1748*.
116. Shah S, Luke JJ, Jacene HA, et al. Results from phase II trial of HSP90 inhibitor, STA-9090 (ganetespib), in metastatic uveal melanoma. *Melanoma Research. 2018;28(6):605-610*.
117. He S, Smith DL, Sequeira M, et al. The HSP90 inhibitor ganetespib has chemosensitizer and radiosensitizer activity in colorectal cancer. *Investigational New Drugs. 2014;32(4):577-586*.
118. Gomez-Casal R, Bhattacharya C, Epperly MW, et al. The HSP90 inhibitor ganetespib radiosensitizes human lung adenocarcinoma cells. *Cancers. 2015;7(2):876-907*.
119. Liu H, Lu J, Hua Y, et al. Targeting heat-shock protein 90 with ganetespib for molecularly targeted therapy of gastric cancer. *Cell Death & Disease. 2015;6(1):e1595*.
120. Wang Y, Liu H, Diao L, et al. Hsp90 Inhibitor Ganetespib Sensitizes Non–Small Cell Lung Cancer to Radiation but Has Variable Effects with Chemoradiation. *Clinical Cancer Research. 2016;22(23):5876-5886*.
121. Forssell-Aronsson E, Bernhardt P, Nilsson O, et al. Biodistribution data from 100 patients iv injected with 111In-DTPA-D-Phe1-octreotide. *Acta Oncologica. 2004;43(5):436-442*.

122. Mazzaglia PJ, Berber E, Milas M, et al. Laparoscopic radiofrequency ablation of neuroendocrine liver metastases: a 10-year experience evaluating predictors of survival. *Surgery. 2007;142(1):10-19*.
123. Kölby L, Bernhardt P, Ahlman H, et al. A transplantable human carcinoid as model for somatostatin receptor-mediated and amine transporter-mediated radionuclide uptake. *The American Journal of Pathology. 2001;158(2):745-755*.
124. Johanson V, Ahlman H, Bernhardt P, et al. A transplantable human medullary thyroid carcinoma as a model for RET tyrosine kinase-driven tumorigenesis. *Endocrine-Related Cancer. 2007;14(2):433-444*.
125. Bolch WE, Eckerman KF, Sgouros G, et al. MIRD pamphlet no. 21: a generalized schema for radiopharmaceutical dosimetry — standardization of nomenclature. *Journal of Nuclear Medicine. 2009;50(3):477-484*.
126. Miller WH, Hartmann-Siantar C, Fisher D, et al. Evaluation of beta-absorbed fractions in a mouse model for 90Y, 188Re, 166Ho, 149Pm, 64Cu, and 177Lu radionuclides. *Cancer Biotherapy & Radiopharmaceuticals. 2005;20(4):436-449*.
127. Dalmo J, Rudqvist N, Spetz J, et al. Biodistribution of 177Lu-octreotate and 111In-minigastrin in female nude mice transplanted with human medullary thyroid carcinoma GOT2. *Oncology Reports. 2012;27(1):174-181*.
128. Dalmo J, Spetz J, Montelius M, et al. Priming increases the anti-tumor effect and therapeutic window of 177Lu-octreotate in nude mice bearing human small intestine neuroendocrine tumor GOT1. *EJNMMI Research. 2017;7(1):6*.
129. Holm S. A simple sequentially rejective multiple test procedure. *Scandinavian Journal of Statistics. 1979:65-70*.
130. Bliss C. The toxicity of poisons applied jointly. *Annals of Applied Biology. 1939;26(3):585-615*.
131. Yeh PJ, Hegreness MJ, Aiden AP, et al. Drug interactions and the evolution of antibiotic resistance. *Nature Reviews Microbiology. 2009;7(6):460-466*.
132. Müller C, Forrer F, Bernard BF, et al. Diagnostic versus therapeutic doses of [177Lu-DOTA-Tyr3]-octreotate: uptake and dosimetry in somatostatin receptor-positive tumors and normal organs. *Cancer Biotherapy & Radiopharmaceuticals. 2007;22(1):151-159*.
133. Schüler E, Österlund A, Forssell-Aronsson E. The amount of injected 177Lu-octreotate strongly influences biodistribution and dosimetry in C57BL/6N mice. *Acta Oncologica. 2016;55(1):68-76*.
134. Bergsma H, Konijnenberg MW, van der Zwan WA, et al. Nephrotoxicity after PRRT with 177Lu-DOTA-octreotate. *European Journal of Nuclear Medicine and Molecular Imaging. 2016;43(10):1802-1811*.
135. Kennedy A, Bester L, Salem R, et al. Role of hepatic intra-arterial therapies in metastatic neuroendocrine tumours (NET): guidelines from the NET-Liver-Metastases Consensus Conference. *HPB. 2015;17(1):29-37*.
136. Rhee TK, Omary RA, Gates V, et al. The effect of catheter-directed CT angiography on yttrium-90 radioembolization treatment of hepatocellular carcinoma. *Journal of Vascular and Interventional Radiology. 2005;16(8):1085-1091*.
137. Milano MT, Constine LS, Okunieff P. Normal tissue tolerance dose metrics for radiation therapy of major organs. *Seminars in Radiation Oncology. 2007;17(2):131-140*.
138. Emami B, Lyman J, Brown A, et al. Tolerance of normal tissue to therapeutic irradiation. *International Journal of Radiation Oncology • Biology • Physics. 1991;21(1):109-122*.
139. Dancey JE, Shepherd FA, Paul K, et al. Treatment of nonresectable hepatocellular carcinoma with intrahepatic 90Y-microspheres. *Journal of Nuclear Medicine. 2000;41(10):1673-1681*.

140. Goin JE, Salem R, Carr BI, et al. Treatment of unresectable hepatocellular carcinoma with intrahepatic yttrium 90 microspheres: factors associated with liver toxicities. *Journal of Vascular and Interventional Radiology. 2005;16(2):205-213*.
141. Gulec SA, Mesoloras G, Dezarn WA, et al. Safety and efficacy of Y-90 microsphere treatment in patients with primary and metastatic liver cancer: the tumor selectivity of the treatment as a function of tumor to liver flow ratio. *Journal of Translational Medicine. 2007;5(15):1-9*.
142. Cremonesi M, Ferrari M, Bodei L, et al. Dosimetry in patients undergoing 177Lu-DOTATATE therapy with indications for 90Y-DOTATATE. *European Journal of Nuclear Medicine and Molecular Imaging. 2006;33(2):S102*.
143. Sandström M, Garske U, Granberg D, et al. Individualized dosimetry in patients undergoing therapy with 177Lu-DOTA-D-Phe1-Tyr3-octreotate. *European Journal of Nuclear Medicine and Molecular Imaging. 2010;37(2):212-225*.
144. Bodei L, Cremonesi M, Grana CM, et al. Peptide receptor radionuclide therapy with 177Lu-DOTATATE: the IEO phase I-II study. *European Journal of Nuclear Medicine and Molecular Imaging. 2011;38(12):2125-2135*.
145. Forssell-Aronsson E, Lanhede B, Fjälling M, et al. Pharmacokinetics and dosimetry of ^{111}In-DTPA-D-Phe^{1}-octreotide in patients with neuroendocrine tumors. *Sixth International Radiopharmaceutical Dosimetry Symposium, Proceedings of a Conference held at Gatlinburg, Tennessee, May 7-10, 1996 (Edited by A Schlafke-Stelson and EE Watson), ORISE 99-0164. 1999;Vol 2:643-654*.
146. Leide-Svegborn S, Nosslin B, Mattsson S. Biokinetics and dosimetry of ^{111}In-DTPA-D-Phe-1-octreotide in patients. *Sixth International Radiopharmaceutical Dosimetry Symposium, Proceedings of a Conference held at Gatlinburg, Tennessee, May 7-10, 1996 (Edited by A Schlafke-Stelson and EE Watson), ORISE 99-0164. 1999;Vol 2:631-642*.
147. Larsson M. Therapy with ^{177}Lu-octreotate – Pharmacokinetics, dosimetry and kidney toxicity [PhD Thesis]: University of Gothenburg, Sweden; 2014.
148. Reynaert H, Rombouts K, Vandermonde A, et al. Expression of somatostatin receptors in normal and cirrhotic human liver and in hepatocellular carcinoma. *Gut. 2004;53(8):1180-1189*.
149. Xidakis C, Mastrodimou N, Notas G, et al. RT-PCR and immunocytochemistry studies support the presence of somatostatin, cortistatin and somatostatin receptor subtypes in rat Kupffer cells. *Regulatory Peptides. 2007;143(1):76-82*.
150. JCGM 100:2008. Evaluation of measurement data – Guide to the expression of uncertainty in measurement. *Joint Committee for Guides in Metrology. 2008*.
151. SFS 2018:506. Dose limits in practices involving ionising radiation. *Swedish Code of Statutes. 2018;Chap 2(§)*.
152. Fueger BJ, Hamilton G, Raderer M, et al. Effects of chemotherapeutic agents on expression of somatostatin receptors in pancreatic tumor cells. *Journal of Nuclear Medicine. 2001;42(12):1856-1862*.
153. Nayak TK, Atcher RW, Prossnitz ER, et al. Enhancement of somatostatin-receptor-targeted 177 Lu-[DOTA 0-Tyr 3]-octreotide therapy by gemcitabine pretreatment-mediated receptor uptake, up-regulation and cell cycle modulation. *Nuclear Medicine and Biology. 2008;35(6):673-678*.
154. Butler LM, Ferraldeschi R, Armstrong HK, et al. Maximizing the therapeutic potential of HSP90 inhibitors. *Molecular Cancer Research. 2015;13(11):1445-1451*.
155. Sharma K, Vabulas RM, Macek B, et al. Quantitative proteomics reveals that Hsp90 inhibition preferentially targets kinases and the DNA damage response. *Molecular & Cellular Proteomics. 2012;11(3):M111.014654*.

156. Dote H, Burgan WE, Camphausen K, et al. Inhibition of hsp90 compromises the DNA damage response to radiation. *Cancer Research. 2006;66(18):9211-9220*.
157. Stingl L, Stühmer T, Chatterjee M, et al. Novel HSP90 inhibitors, NVP-AUY922 and NVP-BEP800, radiosensitise tumour cells through cell-cycle impairment, increased DNA damage and repair protraction. *British Journal of Cancer. 2010;102(11):1578-1591*.
158. Spiegelberg D, Dascalu A, Mortensen AC, et al. The novel HSP90 inhibitor AT13387 potentiates radiation effects in squamous cell carcinoma and adenocarcinoma cells. *Oncotarget. 2015;6(34):35652-35666*.
159. Bergsma H, van Lom K, Raaijmakers MH, et al. Persistent hematologic dysfunction after peptide receptor radionuclide therapy with 177Lu-DOTATATE: incidence, course, and predicting factors in patients with gastroenteropancreatic neuroendocrine tumors. *Journal of Nuclear Medicine. 2018;59(3):452-458*.
160. Forssell-Aronsson E, Nilsson O, Benjegard SA, et al. (111)In-DTPA-D-Phe(1)-octreotide binding and somatostatin receptor subtypes in thyroid tumors. *Journal of Nuclear Medicine. 2000;41(4):636-642*.
161. Waldherr C, Schumacher T, Pless M, et al. Radiopeptide transmitted internal irradiation of non-iodophil thyroid cancer and conventionally untreatable medullary thyroid cancer using [90Y]-DOTA-D-Phe1-Tyr3-octreotide: a pilot study. *Nuclear Medicine Communications. 2001;22(6):673-678*.
162. Bodei L, Handkiewicz-Junak D, Grana C, et al. Receptor radionuclide therapy with 90Y-DOTATOC in patients with medullary thyroid carcinomas. *Cancer Biotherapy and Radiopharmaceuticals. 2004;19(1):65-71*.
163. Iten F, Müller B, Schindler C, et al. Response to [90Yttrium-DOTA]-TOC treatment is associated with long-term survival benefit in metastasized medullary thyroid cancer: a phase II clinical trial. *Clinical Cancer Research. 2007;13(22):6696-6702*.
164. Makis W, McCann K, McEwan AJ. Medullary thyroid carcinoma (MTC) treated with 177Lu-DOTATATE PRRT: a report of two cases. *Clinical Nuclear Medicine. 2015;40(5):408-412*.
165. Vaisman F, de Castro PHR, Lopes FPPL, et al. Is there a role for peptide receptor radionuclide therapy in medullary thyroid cancer? *Clinical Nuclear Medicine. 2015;40(2):123-127*.
166. Salavati A, Puranik A, Kulkarni HR, et al. Peptide receptor radionuclide therapy (PRRT) of medullary and nonmedullary thyroid cancer using radiolabeled somatostatin analogues. *Seminars in Nuclear Medicine. 2016;46(3):215-224*.
167. Leong S, Horoszewicz J, Friedman M, et al. A new cell-line for studies on human thyroid medullary carcinoma. *Proceedings Of The American Association For Cancer Research. 1981;22(49)*.
168. Broutin S, Commo F, De Koning L, et al. Changes in signaling pathways induced by vandetanib in a human medullary thyroid carcinoma model, as analyzed by reverse phase protein array. *Thyroid. 2014;24(1):43-51*.
169. Pfragner R, Wirnsberger G, Niederle B, et al. Establishment of a continuous cell line from a human carcinoid of the small intestine (KRJ-I). *International Journal of Oncology. 1996;8(3):513-520*.
170. Hofving T, Arvidsson Y, Almobarak B, et al. The neuroendocrine phenotype, genomic profile and therapeutic sensitivity of GEPNET cell lines. *Endocrine-Related Cancer. 2018;25(3):367-380*.
171. Evers BM, Townsend Jr CM, Upp JR, et al. Establishment and characterization of a human carcinoid in nude mice and effect of various agents on tumor growth. *Gastroenterology. 1991;101(2):303-311*.
172. Romiani A, Spetz J, Schüler E, et al. Therapeutic potential of Lu-177-octreotate for neuroblastoma – preclinical studies. *NOPHO 35th Annual meeting, Stockholm, Sweden, 2017, poster, PO-59, p 136*.

173. Schmitt A, Bernhardt P, Nilsson O, et al. Biodistribution and dosimetry of 177Lu-labeled [DOTA0, Tyr3] octreotate in male nude mice with human small cell lung cancer. *Cancer Biotherapy and Radiopharmaceuticals. 2003;18(4):593-599*.
174. Schmitt A, Bernhardt P, Nilsson O, et al. Radiation therapy of small cell lung cancer with 177Lu-DOTA-Tyr3-octreotate in an animal model. *Journal of Nuclear Medicine. 2004;45(9):1542-1548*.
175. Wu Y, Pfeifer A, Myschetzky R, et al. Induction of anti-tumor immune responses by peptide receptor radionuclide therapy with 177Lu-DOTATATE in a murine model of a human neuroendocrine tumor. *Diagnostics. 2013;3(4):344-355*.
176. Nonnekens J, van Kranenburg M, Beerens CE, et al. Potentiation of peptide receptor radionuclide therapy by the PARP inhibitor olaparib. *Theranostics. 2016;6(11):1821-1832*.
177. Elf A-K, Bernhardt P, Hofving T, et al. NAMPT inhibitor GMX1778 enhances the efficacy of 177Lu-DOTATATE treatment of neuroendocrine tumors. *Journal of Nuclear Medicine. 2017;58(2):288-292*.
178. Lundsten S, Mortensen A, Mäkiniemi A, et al. The HSP90-inhibitor Onalespib Potentiates 177Lu-Dotatate Treatment of Neuroendocrine Tumors. *European Journal of Nuclear Medicine and Molecular Imaging. 2017;44(Suppl 2):S326*.
179. Lundsten S, Spiegelberg D, Raval N, et al. Potentiating 177Lu-DOTATATE Therapy By HSP90 Inhibition - First In Vivo Study. *European Journal of Nuclear Medicine and Molecular Imaging. 2018;45(Suppl 1):S12*.
180. Spetz J, Langen B, Rudqvist N, et al. Hedgehog inhibitor sonidegib potentiates 177Lu-octreotate therapy of GOT1 human small intestine neuroendocrine tumors in nude mice. *BMC Cancer. 2017;17(1):528*.
181. Pool SE, Bison S, Koelewijn SJ, et al. mTOR inhibitor RAD001 promotes metastasis in a rat model of pancreatic neuroendocrine cancer. *Cancer Research. 2013;73(1):12-18*.
182. Zellmer J, Vomacka L, Boening G, et al. Combination of Peptide Receptor Radionuclide Therapy with Lu-177 DOTATATE and the m-TOR inhibitor RAD001 (Everolimus) in AR42J tumor bearing mice and response assessment by Ga-68 DOTATATE PET. *Journal of Nuclear Medicine. 2018;59(Suppl 1):1346b*.